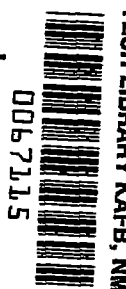


10290
NACA TN 3953



NATIONAL ADVISORY COMMITTEE FOR AERONAUTICS

TECHNICAL NOTE 3953

A LIMITED CORRELATION OF ATMOSPHERIC SOUNDING
DATA AND TURBULENCE EXPERIENCED BY
ROCKET-POWERED MODELS

By Homer P. Mason and William N. Gardner

Langley Aeronautical Laboratory
Langley Field, Va.



Washington

April 1957

AFM C
TECHNICAL LIBRARY
AFL 2011



0067115

NATIONAL ADVISORY COMMITTEE FOR AERONAUTICS

TECHNICAL NOTE 3953

A LIMITED CORRELATION OF ATMOSPHERIC SOUNDING
DATA AND TURBULENCE EXPERIENCED BY
ROCKET-POWERED MODELS

By Homer P. Mason and William N. Gardner

SUMMARY

Atmospheric turbulence as experienced by rocket-powered models and temperature lapse-rate data obtained from rawinsonde soundings have been analyzed and compared in 38 cases by using an assumed temperature lapse-rate stability boundary as a basis for comparison. All the data used in the analysis were obtained from tests made at the Langley Pilotless Aircraft Research Station at Wallops Island, Va.

A limited correlation has been obtained which indicates that atmospheric conditions classified as being unstable will generally be turbulent; however, a marginal or a stable classification does not necessarily indicate smooth air. Thus a large percentage of turbulence can be avoided by making flight tests only during marginal or stable lapse-rate conditions.

INTRODUCTION

The design and operation of both commercial and military aircraft have been seriously complicated by problems associated with atmospheric turbulence. Extensive data have been gathered on such subjects as the gust-load experience of aircraft, the statistical characteristics of turbulence, and aircraft snaking in order to find solutions to some of these problems. References 1 to 11 present examples of some of this work. There have also been numerous attempts to define the meteorological factors associated with atmospheric turbulence - for example, references 12 to 15. As a result of these studies, various parameters have been proposed to aid both the meteorologist and the designer in operational flight planning and in estimating gust-load probability. Most of these parameters have been derived by empirical methods.

A dynamic system responds to random disturbances at the natural frequencies of the system, and the magnitude of the response in any one

mode is primarily a function of the energy in the disturbing elements near the natural frequency of the mode and the amount of damping in the particular mode. In terms of aircraft dynamics, the short-period, or stability-mode, oscillations are excited by random, or noiselike, atmospheric turbulence. Simultaneously, structural modes are excited at their own natural frequencies. The result in terms of acceleration recordings made from an aircraft flying in turbulent air is an oscillatory trace near the stability-mode natural frequency with one or more superimposed structural vibrations. (See ref. 1.) The stability-mode oscillation may be distorted from a true sine-wave oscillation in both frequency and amplitude.

This distortion of the stability mode by rough air can seriously affect the accuracy with which dynamic data, particularly damping and buffeting data, can be obtained for research purposes. Indeed, this distortion can make the identification of buffeting very difficult, if not impossible, when an aircraft is flying in rough air. The problem of the effects of atmospheric turbulence on aircraft has recently been encountered in tests of rocket-powered research models. It has thus become important for investigators to be able to select flight-test conditions which will yield the most reliable data.

Atmospheric soundings are routine in connection with flight tests of rocket-powered models conducted by the National Advisory Committee for Aeronautics. The soundings are made as near to the actual flight time and flight path as is practical by releasing a rawinsonde from the launching site, usually withing less than 1 hour of the flight test. A comparison of these atmospheric sounding data with the occurrence of turbulence, as indicated by roughness on telemeter records of acceleration and angle of attack, is presented herein for 38 tests conducted from 1952 to 1955 at the Langley Pilotless Aircraft Research Station at Wallops Island, Va. The purpose of this paper is to present an approximate criterion which may be used, in the absence of qualified meteorological assistance, as an aid in the selection of atmospheric conditions which are suitable to the turbulence requirements of a flight test. To this end, particular attention will be focused on a correlation of atmospheric temperature lapse rate and the occurrence of turbulence.

SYMBOLS

a_n	normal acceleration, g units
a_t	transverse acceleration, g units

α angle of attack, deg
h altitude, ft
M Mach number

MODELS AND TESTS

Small sketches included in each of figures 1 to 38 show the approximate configurations of the rocket models from which data were obtained for this correlation. With the exception of the models shown in figures 1 and 2, each of the models was designed and instrumented for investigation of aerodynamic problems other than atmospheric turbulence. Those shown in figures 1 and 2 were designed and instrumented specifically for the investigation of gust loads reported in reference 1.

All the models were accelerated to near-sonic or supersonic speeds by external booster-rocket motors. In some cases, internal rocket motors were incorporated to sustain or increase the model speed after separation from the external booster. Model velocity and flight-path data were obtained from a CW Doppler radar set and a modified SCR-584 tracking radar unit. Acceleration and angle-of-attack data were obtained by telemetering the instrument readings from the models to a ground receiving station. Test Reynolds numbers were of the order of 10×10^6 .

Rawinsonde soundings to obtain atmospheric data were conducted in conjunction with each flight test. Rawinsondes were released from the test site at a time as near as practical to the time the test model was launched (usually within less than 1 hour).

All tests were conducted at the Langley Pilotless Aircraft Research Station at Wallops Island, Va., during afternoon hours when the sky was generally clear of large cloud formations, there was no precipitation, and visibility was virtually unlimited.

PRESENTATION OF DATA

Data pertinent to the analysis are presented in figures 1 to 38. The rocket-model tests from which data have been used were selected on the basis of the current availability of the original flight records and the instrumentation of the models. Only those models which contained either accelerometers or angle-of-attack indicators, or both, are included herein, and most of the models also contained other instrumentation. Some of the available data have been rejected because the

flight-test program for these models required intentional flight-path disturbances. The presence of these intentional disturbances on the flight records makes the identification of turbulence very difficult; therefore, these data have been considered unacceptable for correlation purposes.

Model Data

The rocket-model data used in the analysis are shown on the right-hand side of each figure. At the top of the figures is a tracing of a representative sample of the actual flight record. In several of the figures, two samples of the telemeter records of acceleration are shown to illustrate the differences between what is identified as turbulence response of the model and what is not. At the bottom of the figures is a time history of the altitude and Mach number of the model. The time histories are limited to the first 20 seconds of flight time and Mach numbers greater than 0.8.

Hatched bands are superimposed on the altitude plots to indicate the times and the altitudes at which turbulence was identified. No turbulence has been indicated in any case while the model was being accelerated by its booster-rocket motor because vibration characteristics of external booster-rocket motors are such as to mask the turbulence effects which may be experienced during the boosted portions of the model flights. The internal rocket motors which are generally used as sustainer motors do not have as severe vibration characteristics as the external booster motors. Consequently, turbulence experienced during acceleration of the models after booster separation has been indicated in those cases where it could be clearly identified.

The width of the turbulence bands shown in the figures varies approximately as the magnitude of the turbulence indicated; however, no values of magnitude, or turbulence intensity, are implied by the width of these bands. Comparison of the turbulence intensity experienced in one test with that experienced in another test is not possible because of the wide variation of configurations, wing loadings, Mach numbers, and instrument ranges in the various tests. Except for the models used in figures 1 and 2, the instrument ranges and response characteristics were probably not optimum for quantitative indications of atmospheric turbulence, and the turbulence indications obtained were only incidental to the purpose of the tests. In general, the telemeter tracings of the present investigation indicated less than about $\pm 2g$ acceleration or $\pm 1^\circ$ angle-of-attack excursions attributable to atmospheric turbulence.

Atmospheric Sounding Data

On the left-hand side of each figure is a copy of a portion of the standard USAF skew T, log p diagram on which is plotted the temperature against pressure as determined in each test from the rawinsonde sounding. The pressure and temperature data shown were faired through approximately 25 contact points between the ground and the 700 millibar pressure level; therefore, these data are considerably more detailed than data normally available from routine weather sequence reports. Wind direction and wind speed, where available, are also shown in each figure at the appropriate pressure altitude. Wind direction is specified in accordance with a 16-point compass rose and wind speed is given in feet per second. The pressure scale on the rawinsonde sounding plots and the altitude scale on the model time-history plots are aligned so that it is possible to read directly across each figure from pressure to altitude.

ANALYSIS OF DATA

Model Data

Figures 1 and 2 present data which were obtained from models designed for a gust-load investigation and which were flight tested under conditions known to be turbulent. A piloted airplane was used for an atmospheric survey prior to flight tests of the models, and the models were not flown until moderate turbulence was known to exist. The technique used in these tests and data from similar tests are presented in reference 1. The models used in the tests of figures 1 and 2 were symmetrical and experienced no intentional disturbances other than the turbulent atmosphere through which they were flown. Thus the data obtained from these models are illustrative of the response of an aircraft to atmospheric turbulence. The excitation of the short-period stability mode with distortion of the wave shape and the superimposed structural vibrations are characteristic of turbulence response. These general characteristics will be present whenever an aircraft flies through turbulent air, and the magnitude of the response in any one mode will be dependent on the strength of the turbulence, the speed of the aircraft, the aerodynamics of the configuration, and the structure of the airframe.

Although the turbulence indicated in figures 1 and 2 was more severe than would be expected during routine rocket-model tests, the data obtained from these models have been used as a guide in determining the appearance of turbulence on the flight records presented in figures 3 to 38. The data shown in figures 3 to 38 are representative of routine rocket-model tests, which usually are made only during relatively calm weather when good photographic records can be obtained.

Inasmuch as the characteristics of any turbulence indicated by these data are not known, the present analysis is limited only to a consideration of whether or not noticeable and recognizable turbulence was present during the flight tests of the models. If the records obtained from a flight test show that the model was excited unintentionally and that an irregular oscillation in a stability mode developed, with superimposed random structural frequencies, then the motion is considered to be a response to turbulence in the atmosphere along the model flight path.

Atmospheric Sounding Data

The static-pressure, temperature, and wind-velocity data presented herein were the only data obtained from the atmospheric soundings. It is recognized that these data are insufficient for a complete analysis of the meteorological factors associated with atmospheric turbulence. However, two of the several factors known to affect atmospheric turbulence are available: (1) the lapse rate, which is the rate of variation of atmospheric temperature with altitude, and (2) the wind gradient, which is the rate of variation of wind direction and speed with altitude (refs. 16 to 18). As previously stated, the purpose of this report is to compare the lapse rate and wind gradient with the occurrence of atmospheric turbulence as encountered in rocket-model tests for the specific purpose of determining a method whereby test conditions can be selected in accordance with the atmospheric-turbulence requirements of the test to be made. Temperature lapse-rate data usually are more readily available than are wind data because of the considerable time required to compute wind data. Thus, it is logical to consider temperature lapse-rate data first.

References 16 to 18 show that a temperature lapse rate corresponding to that of a dry parcel of air transported vertically, referred to as the dry adiabatic lapse rate, is clearly unstable. The term "unstable" means that if this parcel of air is displaced from an initial altitude it will continue to move in the direction of the displacement. Conversely, the lapse rate corresponding to that of a parcel of saturated air transported vertically, the wet adiabatic lapse rate, is clearly stable. These statements apply below the convective condensation levels when no clouds are formed.

Since only the extremes of wet or dry adiabatic lapse rates appear to be conclusive indicators of atmospheric stability when other factors are not considered and since physical processes are seldom sharply discontinuous, it becomes necessary to assume some lapse-rate criteria between these limits for correlation of lapse-rate data with the occurrence of atmospheric turbulence. In the present analysis a lapse rate approximately midway between the average wet and dry adiabatic lines in

the appropriate pressure and temperature ranges has been assumed to be a stability boundary. This boundary is shown on each of figures 1 to 38 as a dashed line on the sounding plots and in each instance was determined primarily by visual inspection. Average measured lapse rates which are greater or drier than this boundary are assumed to be unstable, and similarly, average measured lapse rates which are less or wetter than this boundary are assumed to be stable. A measured lapse rate which is near the assumed stability boundary is considered to be marginal. Throughout this analysis an unstable lapse rate is considered to be indicative of atmospheric turbulence and a stable lapse rate indicative of smooth air.

Limitations of Data

In applying the criteria of the preceding section, the accuracy of the temperature data and the possible altitude discrepancies between the rocket-model data and the sounding data should be considered. Reference 19 shows that temperature data obtained from rawinsondes is accurate to within approximately 1°C and that the altitude of the rawinsondes can be determined to within approximately 150 feet at the 700-millibar pressure level. Above this altitude the accuracy decreases. Model altitudes obtained from radar data are believed to be accurate to within about 50 feet at moderate ranges. Because of the time lapse between the sounding data and the rocket-model data, which is usually less than 1 hour, changes of atmospheric characteristics with time could contribute to further inaccuracies in the determination of the altitude at which a given characteristic occurs. Thus it is believed that altitude discrepancies between rocket-model and sounding data may sometimes be as great as 500 feet. In most cases, however, the elapsed time and the rate of change of atmospheric conditions with time are believed to be small enough to allow an altitude discrepancy of no more than 250 feet.

The present correlation is limited to altitudes below about 10,000 feet or the 700-millibar pressure level because of the following circumstances: A large majority of the rocket-model data presented herein were obtained below about 10,000 feet. The various factors that may affect turbulence but have been neglected in this analysis might be expected to have a more important influence at altitudes greater than 10,000 feet than at lower levels. Inaccuracies between rocket-model and rawinsonde data that result from deviations of the rawinsonde from the model flight path would be greater at higher altitudes. Finally, strong temperature inversions and large, nearly isothermal variations with altitude are not considered in the correlation of the average lapse rates over the altitude range in question because an inversion is generally very stable and exerts a damping action on turbulence originating

below the inversion. The extent to which turbulence can penetrate an inversion depends on properties of the air mass which were not determined in this investigation.

Application of Analysis

Three figures have been arbitrarily selected to illustrate the application of the preceding methods of analysis (figs. 4, 28, and 37). In figure 4 two samples of the flight records are shown. The first sample shows irregular oscillations in both normal and transverse acceleration which have frequencies corresponding to the short-period natural pitch and yaw stability modes for the configuration. Superimposed on these oscillations are random disturbances which have a frequency near the first bending frequency of the model tail fins. Thus, in accordance with the previously outlined criteria, this section of model telemeter record is considered to be indicative of the fact that the model was flying in turbulent air. The second sample of record is comparatively smooth and thus is considered to indicate that the model was flying in smooth air. The various periods of turbulent and smooth air noted throughout the flight record have been indicated at the appropriate times on the altitude time-history curve. In figures 28 and 37 the samples of flight records shown are also comparatively smooth and each of these models is considered to have experienced smooth air. Turbulence was not experienced at any time during the flight of these two models.

In examining the atmospheric sounding data the first step is to determine a temperature lapse-rate stability boundary. The lines on the sounding plots which represent wet and dry adiabatic expansion are curved; however, at altitudes below the 700-millibar pressure level they can be assumed to be straight. If this assumption is made, it is a simple procedure to determine a line which bisects the angle between the particular wet and dry adiabatic lines that constitute general limits of the sounding data. This line then represents an assumed stability boundary. A visual comparison of the lapse rate of the assumed stability boundary with the measured data indicates that figure 4 represents an unstable atmospheric condition because the measured average temperature lapse rate below the inversion is greater, or dryer, than that of the assumed stability boundary. In figure 28 the average measured lapse rate is approximately the same as that of the assumed stability boundary, and in figure 37 the average measured lapse rate is less, or wetter, than that of the assumed stability boundary. Therefore, in accordance with the previously stated criteria, turbulence would be expected in the atmosphere represented in figure 4, whereas the atmosphere represented in figure 28 would be expected to be marginal and turbulence might or might not be present. Figure 37 represents a

stable atmosphere in which turbulence would not be expected. As previously discussed, the rocket model of figure 4 experienced turbulent air whereas the models of figures 28 and 37 did not.

It is expected that any correlation of turbulence experience based only on the preceding temperature lapse-rate criteria will leave much to be desired. If, however, a simple inspection of easily obtained lapse-rate data can be used as illustrated herein to indicate the presence of atmospheric turbulence in a significant number of cases, even if they are only extreme or unusual cases, the purpose of this investigation will be fulfilled.

RESULTS AND DISCUSSION

The data presented in figures 1 to 38 have been analyzed in accordance with the preceding methods of analysis and the results are summarized in table I. The X symbols indicate the classification of the data presented in each figure. As noted in the table, the data have been arranged in three distinct groups according to the unstable, marginal, or stable classification of the atmosphere. Within each of the three general groups, those cases in which turbulence was experienced are listed first. In the last column, X symbols are shown for variations of wind direction greater than about 90° or wind-speed gradients of approximately 15 feet per second per 1,000 feet of altitude below 10,000 feet. A dash indicates that wind data were not available.

Of the 38 cases selected for this analysis, the atmospheric conditions were considered to be unstable in 19 cases, marginal in 10 cases, and stable in 9 cases. Atmospheric turbulence was experienced by the rocket models in 18 (95 percent) of the unstable cases, in 5 (50 percent) of the marginal cases, and in 4 (44 percent) of the stable cases. Thus the present analysis would seem to indicate that atmospheric conditions which are classified as being unstable will generally be turbulent, whereas a marginal or a stable classification does not necessarily indicate smooth air. Therefore, by using the turbulence criteria specified herein for selecting atmospheric conditions suitable for rocket-model flight tests, a large percentage of the turbulent atmospheric conditions could be avoided. The quality and reliability of the aerodynamic data obtained from rocket-model tests should be correspondingly improved. Qualified meteorological assistance should be obtained for selecting atmospheric conditions in those instances where ideally smooth air is desired for a given flight test.

Even though wind data are not available for each case, there does not appear to be any obvious correlation between wind data and turbulence experience for the conditions of this analysis. In most cases

the wind gradients experienced were caused by changes in wind direction only, inasmuch as the velocity gradients were generally small.

It may be interesting to note that in two instances two models were flown during the same afternoon with an elapsed time interval of approximately $1\frac{1}{2}$ hours. An atmospheric sounding was made in each case during the elapsed time interval. In both instances the atmosphere has been classified as unstable, and turbulence was experienced by each of the four rocket models. The first instance is represented by the models in figures 3 and 4, and the second instance by the models in figures 15 and 16.

CONCLUDING REMARKS

The occurrence of atmospheric turbulence as indicated by telemeter records obtained from rocket-powered model flight tests has been correlated with the stability of atmospheric temperature lapse rates as obtained from rawinsonde sounding data. The unstable, marginal, or stable classification of average measured temperature lapse rate has been made in accordance with an assumed lapse-rate stability boundary which is midway between the wet and dry adiabatic lines that constitute general limits of a particular atmospheric sounding plot made on a standard USAF skew T, log p diagram. All the data used in the correlation were obtained from tests made at the Pilotless Aircraft Research Station at Wallops Island, Va., during afternoon hours when the sky was generally clear of large cloud formations, there was no precipitation, and visibility was virtually unlimited. Analysis of the data is limited to altitudes below 10,000 feet or below strong temperature inversions or isothermal layers.

The analysis indicates that atmospheric conditions which are classified as being unstable will generally be turbulent; however, a marginal or a stable classification does not necessarily indicate smooth air. Thus, a large percentage of the turbulent atmospheric conditions which can invalidate flight-test data may be avoided by a simple inspection of temperature lapse-rate data.

Langley Aeronautical Laboratory,
National Advisory Committee for Aeronautics,
Langley Field, Va., December 19, 1956.

REFERENCES

1. Vitale, A. James, Press, H., and Shufflebarger, C. C.: An Investigation of the Use of Rocket-Powered Models for Gust-Load Studies With an Application to a Tailless Swept-Wing Model at Transonic Speeds. NACA TN 3161, 1954.
2. Coleman, Thomas L., Copp, Martin R., Walker, Walter G., and Engel, Jerome N.: An Analysis of Accelerations, Airspeeds, and Gust Velocities From Three Commercial Operations of One Type of Medium-Altitude Transport Airplane. NACA TN 3365, 1955.
3. McDougal, Robert L., Coleman, Thomas L., and Smith, Philip L.: The Variation of Atmospheric Turbulence With Altitude and Its Effect on Airplane Gust Loads. NACA RM L53G15a, 1953.
4. Mazelsky, Bernard: Charts of Airplane Acceleration Ratio for Gusts of Arbitrary Shape. NACA TN 2036, 1950.
5. Langley Gust Loads Branch: Notes on the Gust Problem for High-Speed Low-Altitude Bombers. NACA RM L52E22, 1952.
6. Burns, Anne: Notes on the Dynamic Response of an Aircraft to Gusts and on the Variation of Gust Velocity Along the Flight Path With Special Reference to Measurements Made in Lancaster P.D. 119. R. & M. No. 2759, British A.R.C., Sept. 1949.
7. Diederich, Franklin Wolfgang: The Response of an Airplane to Random Atmospheric Disturbances. Ph. D. Thesis, C.I.T., 1954.
8. Press, Harry, Meadows, May T., and Hadlock, Ivan: A Reevaluation of Data on Atmospheric Turbulence and Airplane Gust Loads for Application in Spectral Calculations. NACA Rep. 1272, 1956. (Supersedes NACA TN 3362 by Press, Meadows, and Hadlock and TN 3540 by Press and Meadows.)
9. Zbrożek, J. K.: A Study of the Longitudinal Response of Aircraft to Turbulent Air. Rep. No. Aero. 2530, British R.A.E., Jan. 1955.
10. Bird, John D.: Some Calculations of the Lateral Response of Two Airplanes to Atmospheric Turbulence With Relation to the Lateral Snaking Problem. NACA TN 3425, 1955. (Supersedes NACA RM L50F26a.)
11. Cahill, Jones F., and Bird, John D.: Low-Speed Tests of a Free-To-Yaw Model in Two Wind Tunnels of Different Turbulence. NACA RM L51L14, 1952.

12. Donely, Philip: Effective Gust Structure at Low Altitudes as Determined From the Reactions of an Airplane. NACA Rep. 692, 1940.
13. Halstead, Maurice H.: The Relationship Between Wind Structure and Turbulence Near the Ground. Supplement to Interim Rep. No. 14, Apr. 1, 1951 - June 30, 1951, The Johns Hopkins Univ., Lab. of Climatology (Seabrook, N. J.), June 30, 1951.
14. Thompson, James K.: A Relation of Wind Shear and Insolation to the Turbulence Encountered by an Airplane in Clear-Air Flight at Low Altitudes. NACA RM L51H07, 1951.
15. Summers, Robert A.: A Statistical Description of Large-Scale Atmospheric Turbulence. Sc. D. Thesis, M.I.T., 1954. (Also Rep. T-55, Instrumentation Lab., M.I.T., May 17, 1954.)
16. Petterssen, Sverre: Weather Analysis and Forecasting. McGraw-Hill Book Co., Inc., 1940.
17. Byers, Horace Robert: Synoptic and Aeronautical Meteorology. McGraw-Hill Book Co., Inc., 1937.
18. Gregg, Willis Ray: Aeronautical Meteorology. Second ed., The Ronald Press Co., 1930.
19. Anon.: Accuracies of Radiosonde Data. AWS Tech. Rep. 105-133, Military Air Transport Service, U. S. Air Force, Sept. 1955.

TABLE I

SUMMARY OF ROCKET MODEL AND ATMOSPHERIC SOUNDING DATA¹

Figure	Turbulence indicated by model	Average lapse rate unstable	Average lapse rate marginal	Average lapse rate stable	Appreciable wind gradients present
1	X	X			-
2	X	X			
3	X	X			X
4	X	X			X
5	X	X			
6	X	X			-
7	X	X			X
8	X	X			-
9	X	X			
10	X	X			
11	X	X			-
12	X	X			-
13	X	X			-
14	X	X			X
15	X	X			-
16	X	X			-
17	X	X			X
18	X	X			
19		X			
20	X		X		X
21	X		X		X
22	X		X		
23	X		X		X
24	X		X		-
25			X		-
26			X		-
27			X		X
28			X		X
29			X		X
30	X			X	X
31	X			X	X
32	X			X	-
33	X			X	-
34				X	X
35				X	-
36				X	X
37				X	
38				X	-

¹An X indicates classification of the data; a dash indicates that data are not available.

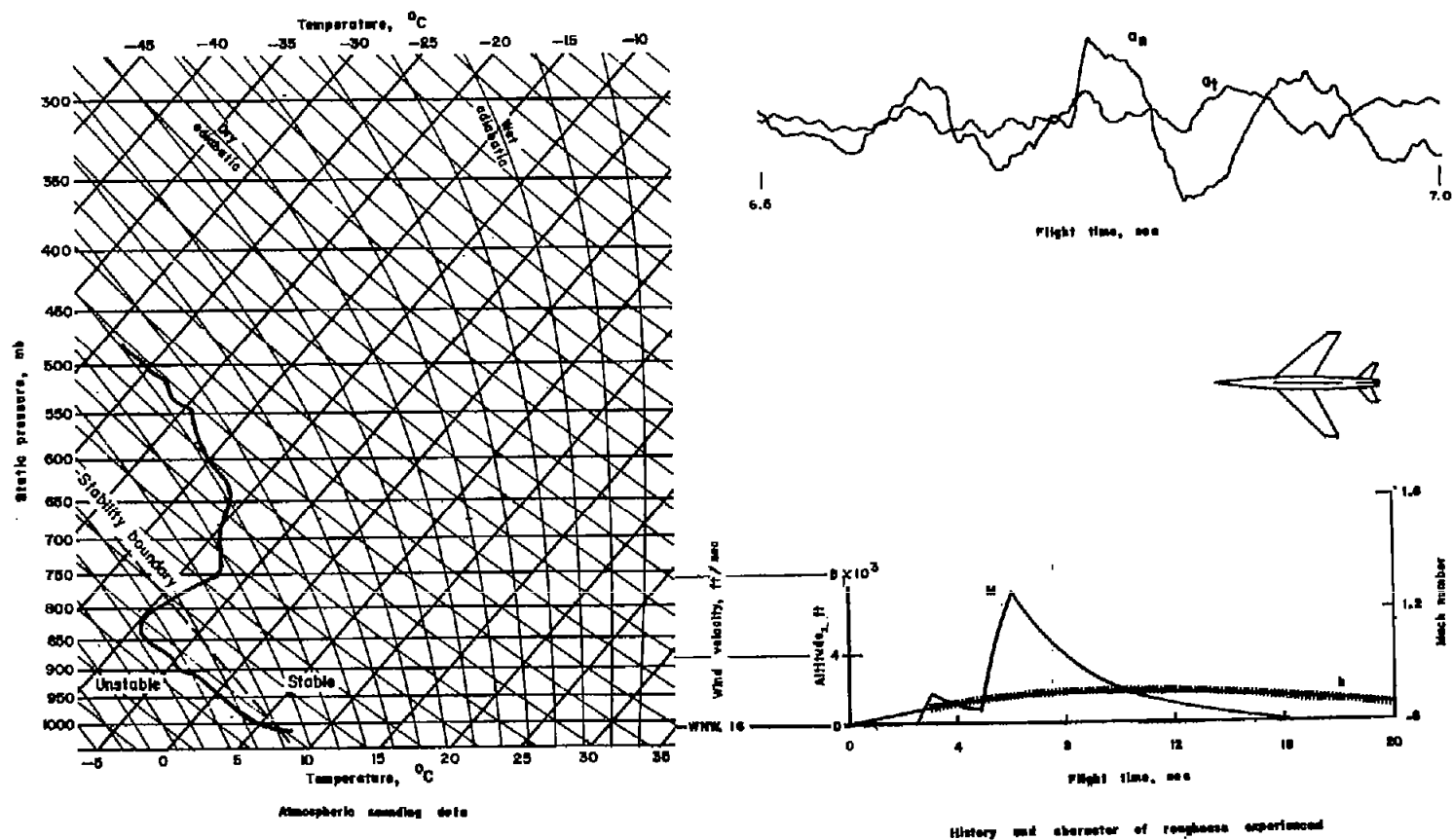


Figure 1.- Flight test made on March 28, 1955, with rawinsonde released at 2:15 p. m. (e. s. t.).
Model flown under conditions known to be turbulent with a wing loading of 24 lb/sq ft.

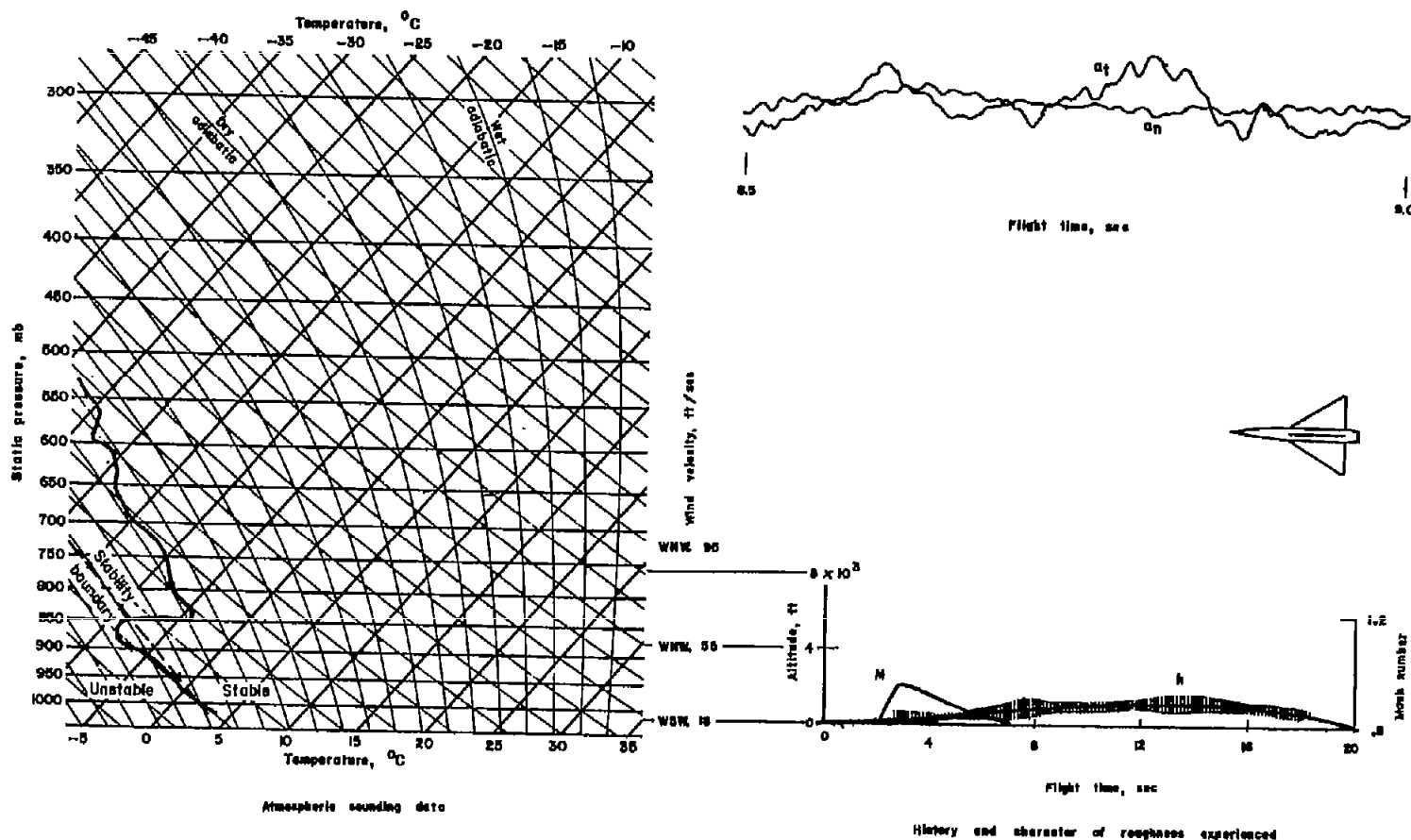


Figure 2.- Flight test made on January 28, 1954, with rawinsonde released at 2:30 p. m. (e. s. t.) and model launched at 2:17 p. m. (e. s. t.). Model flown under conditions known to be turbulent with a wing loading of 24 lb/sq ft.

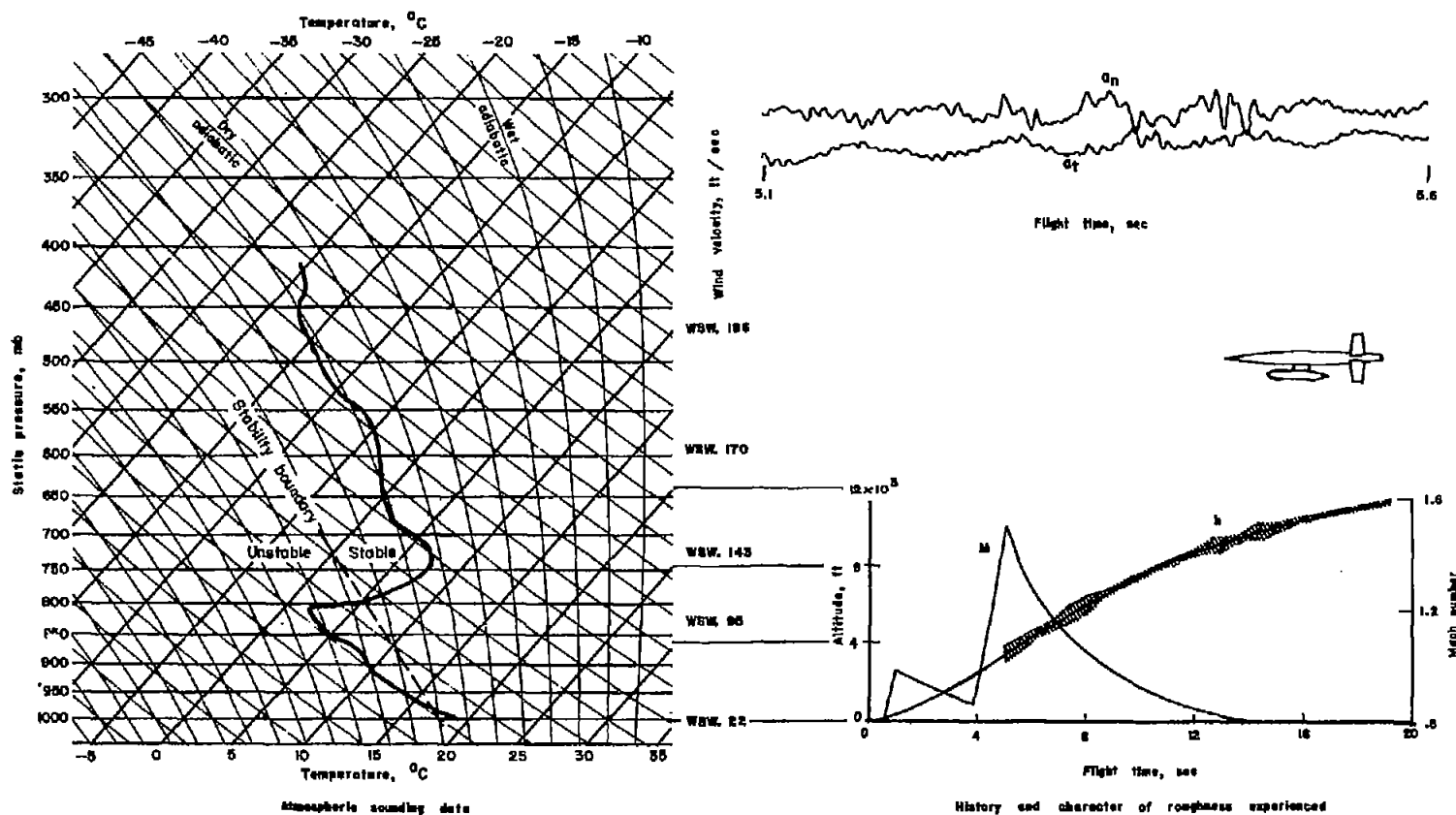


Figure 3.- Flight test made on December 14, 1953, with rawinsonde released at 2:56 p. m. (e. s. t.) and model launched at 4:00 p. m. (e. s. t.). Model wing loading, 58 lb/sq ft.

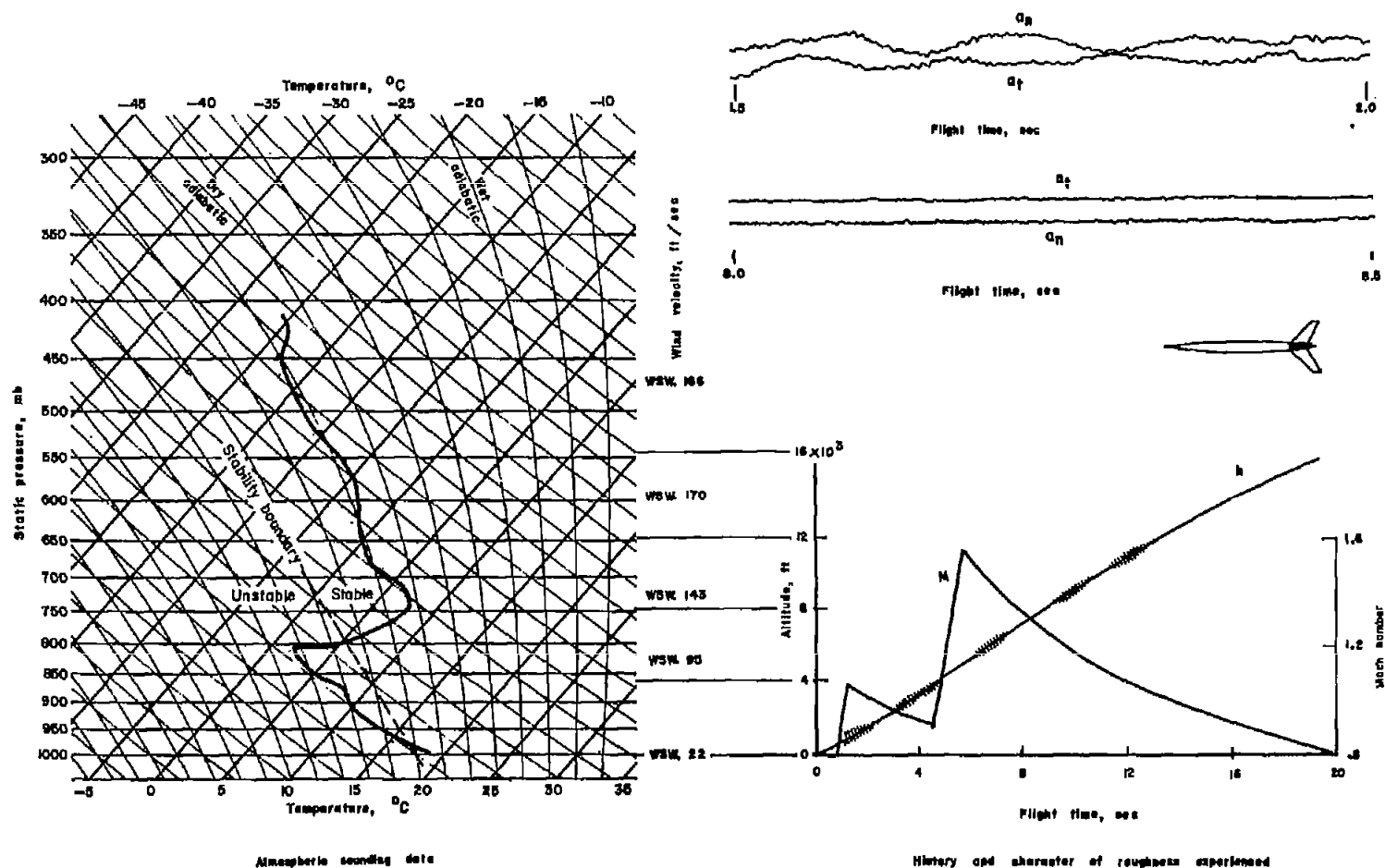


Figure 4.- Flight test made on December 14, 1953, with rawinsonde released at 2:56 p. m. (e. s. t.) and model launched at 3:27 p. m. (e. s. t.). Model wing loading, 68 lb/sq ft.

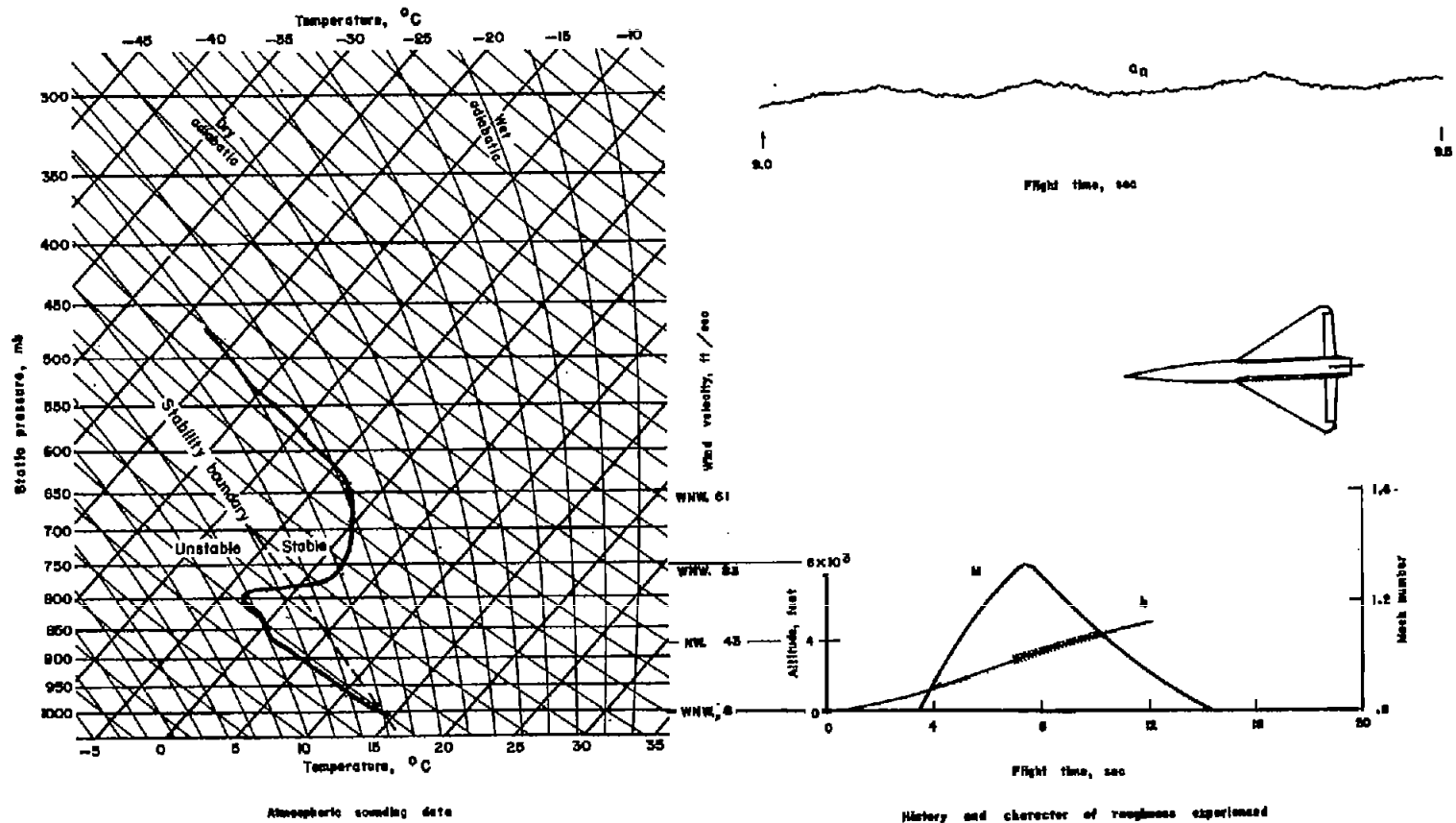


Figure 5.- Flight test made on February 25, 1954, with rawinsonde released at 3:06 p. m. (e. s. t.) and model launched at 2:48 p. m. (e. s. t.). Model wing loading, 19 lb/sq ft.

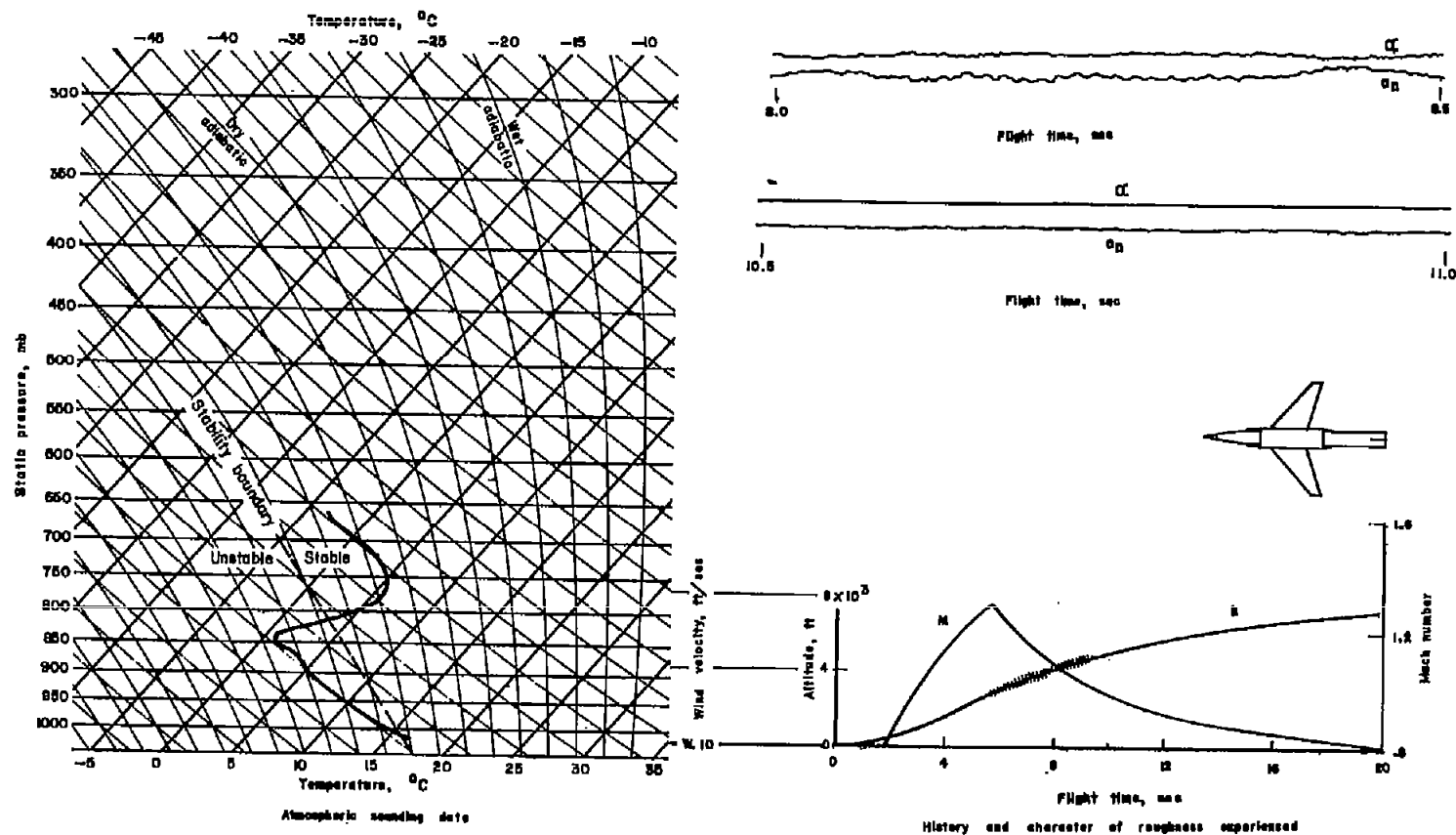


Figure 6.- Flight test made on March 16, 1953, with rawinsonde released at 3:14 p. m. (e. s. t.).
Model wing loading, 28 lb/sq ft.

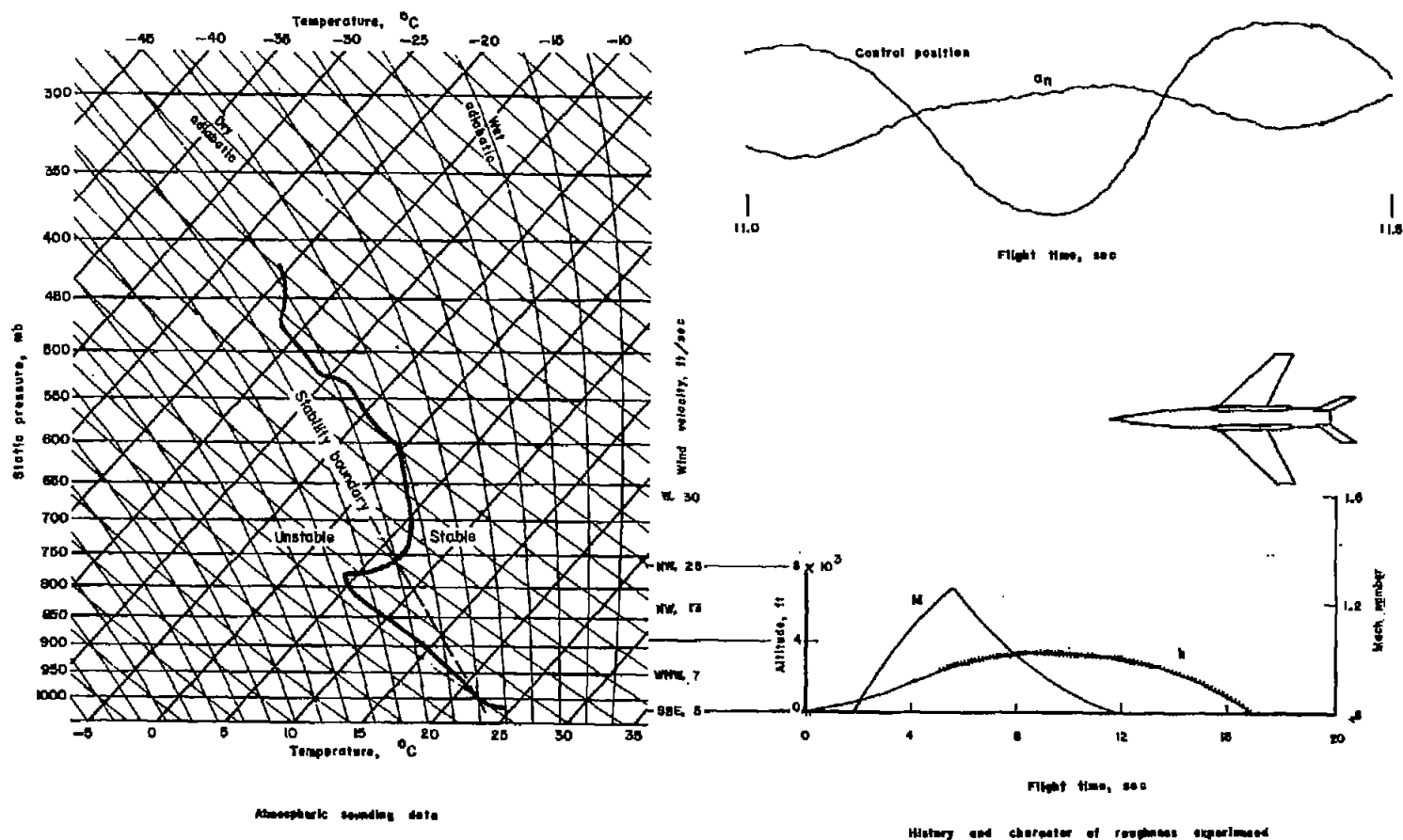


Figure 7.- Flight test made on August 19, 1953, with rawinsonde released at 2:48 p. m. (e. s. t.) and model launched at 2:55 p. m. (e. s. t.). Model wing loading, 45 lb/sq ft.

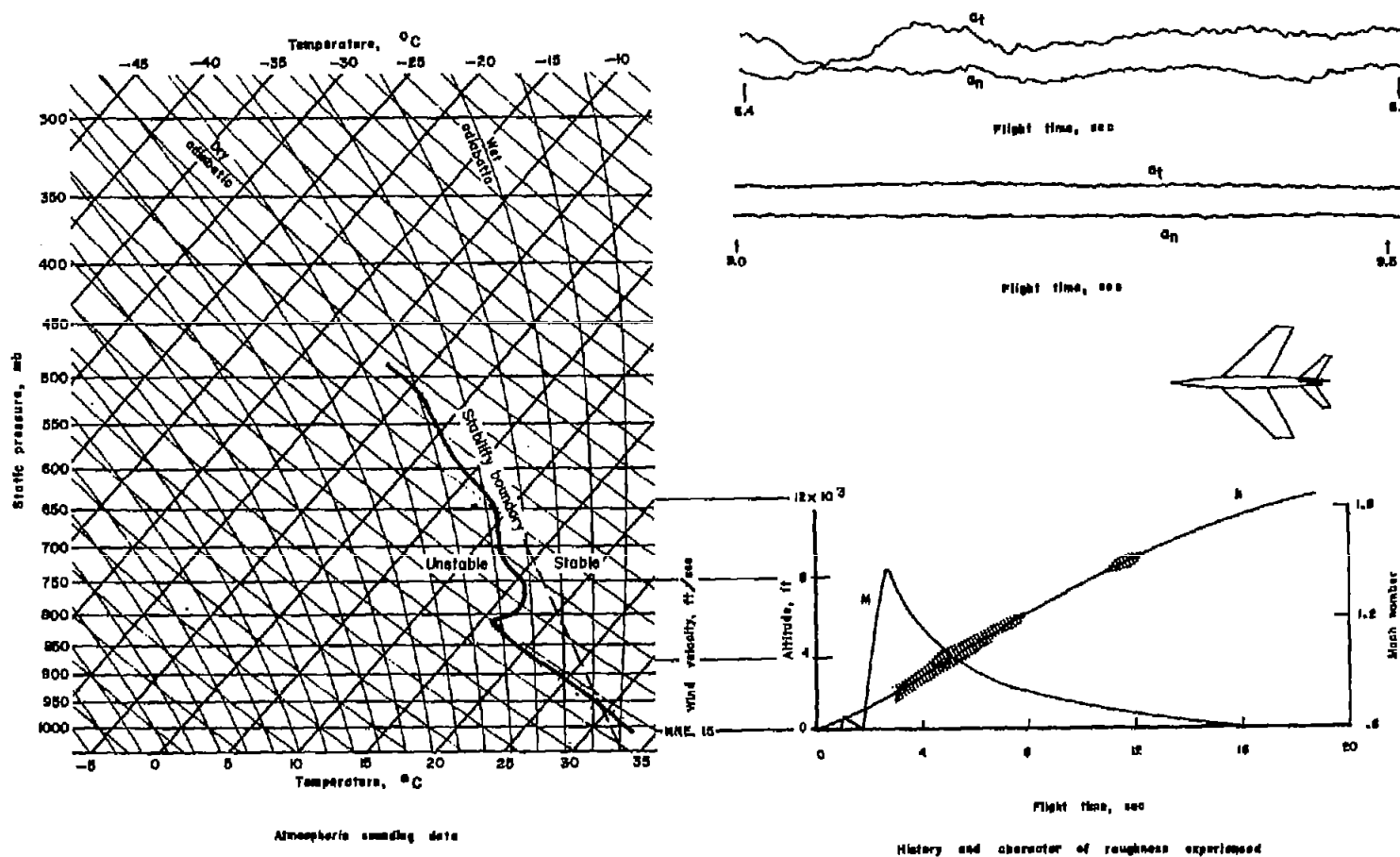


Figure 8.- Flight test made on June 18, 1952, with rawinsonde released at 3:49 p. m. (e. s. t.) and model launched at 2:58 p. m. (e. s. t.). Model wing loading, 21 lb/sq ft.

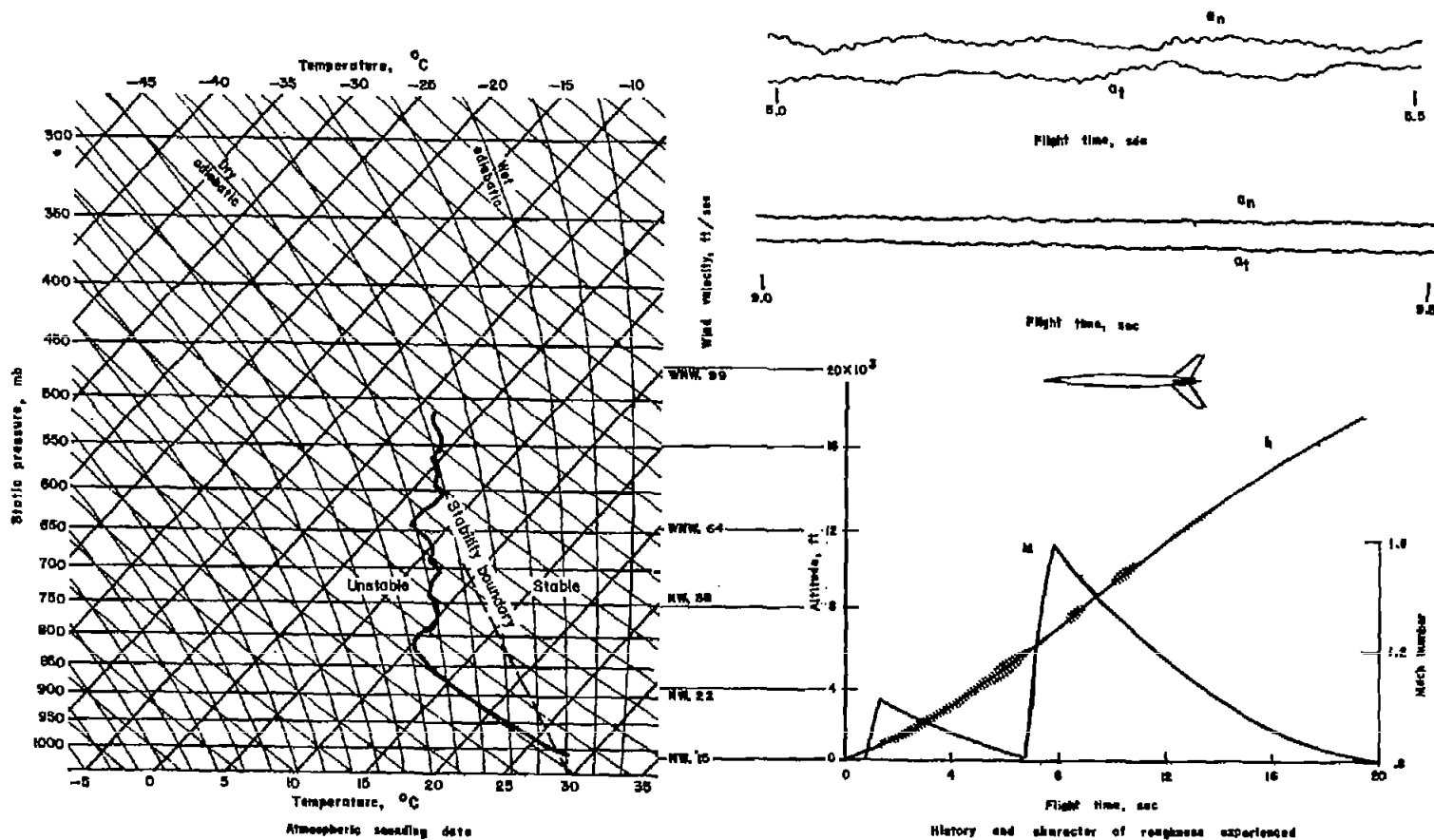


Figure 9.- Flight test made on July 23, 1954, with rawinsonde released at 3:14 p. m. (e. s. t.) and model launched at 3:01 p. m. (e. s. t.). Model wing loading, 57 lb/sq ft.

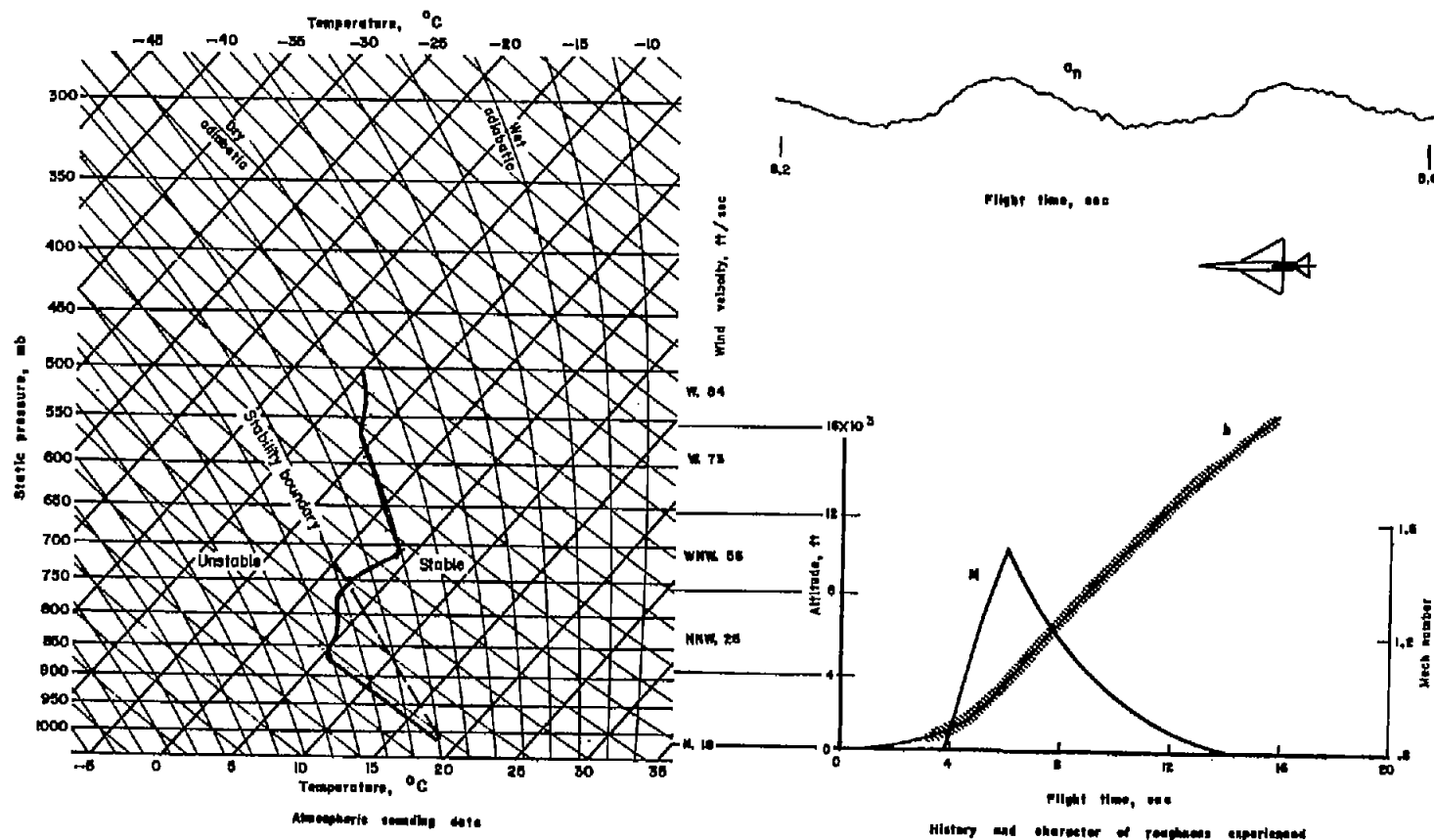


Figure 10.- Flight test made on September 22, 1953, with rawinsonde released at 12:40 p. m. (e. s. t.). Model wing loading, 27 lb/sq ft.

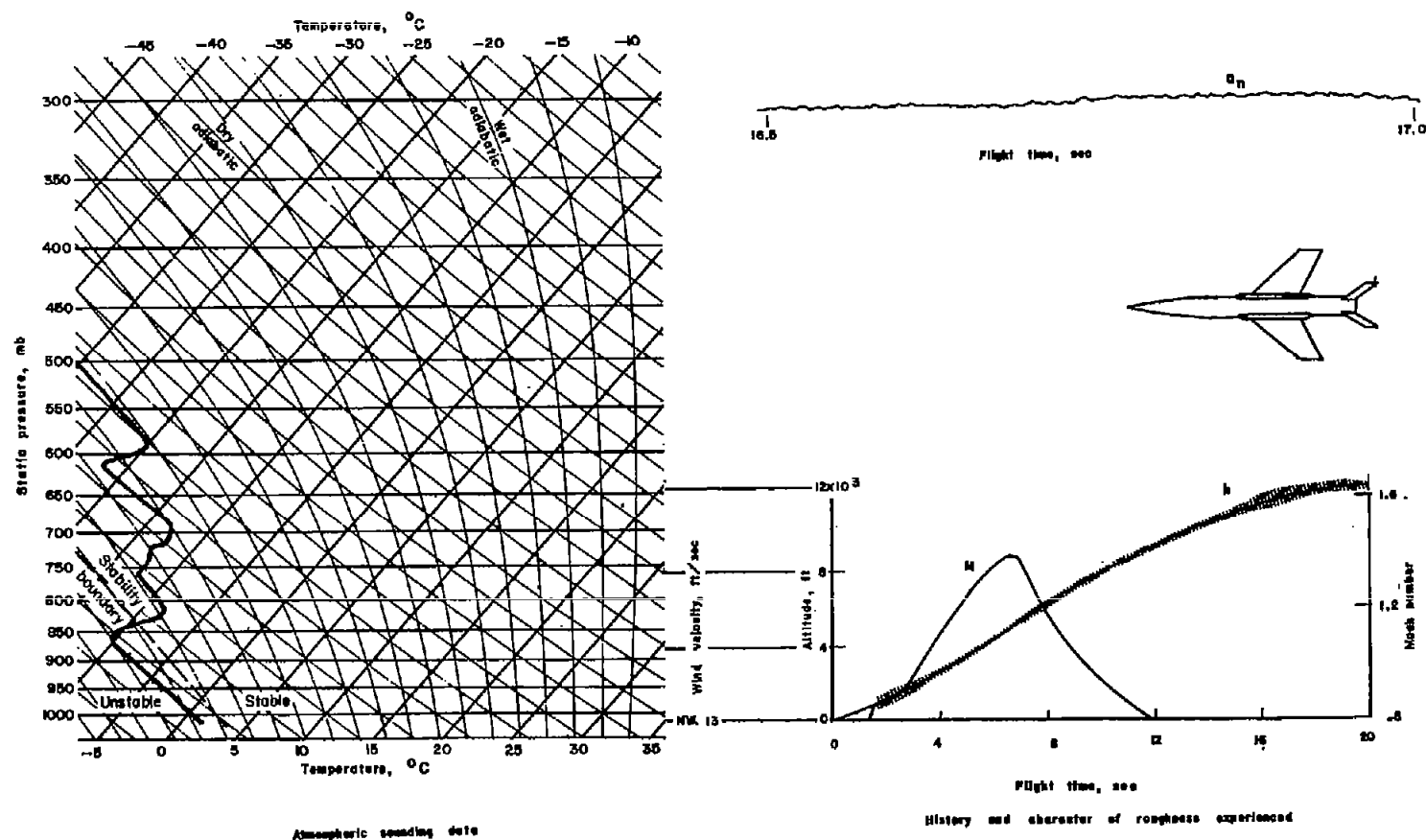


Figure 11.- Flight test made on December 15, 1952, with rawinsonde released at 2:08 p. m. (e. s. t.) and model launched at 3:00 p. m. (e. s. t.). Model wing loading, 45 lb/sq ft.

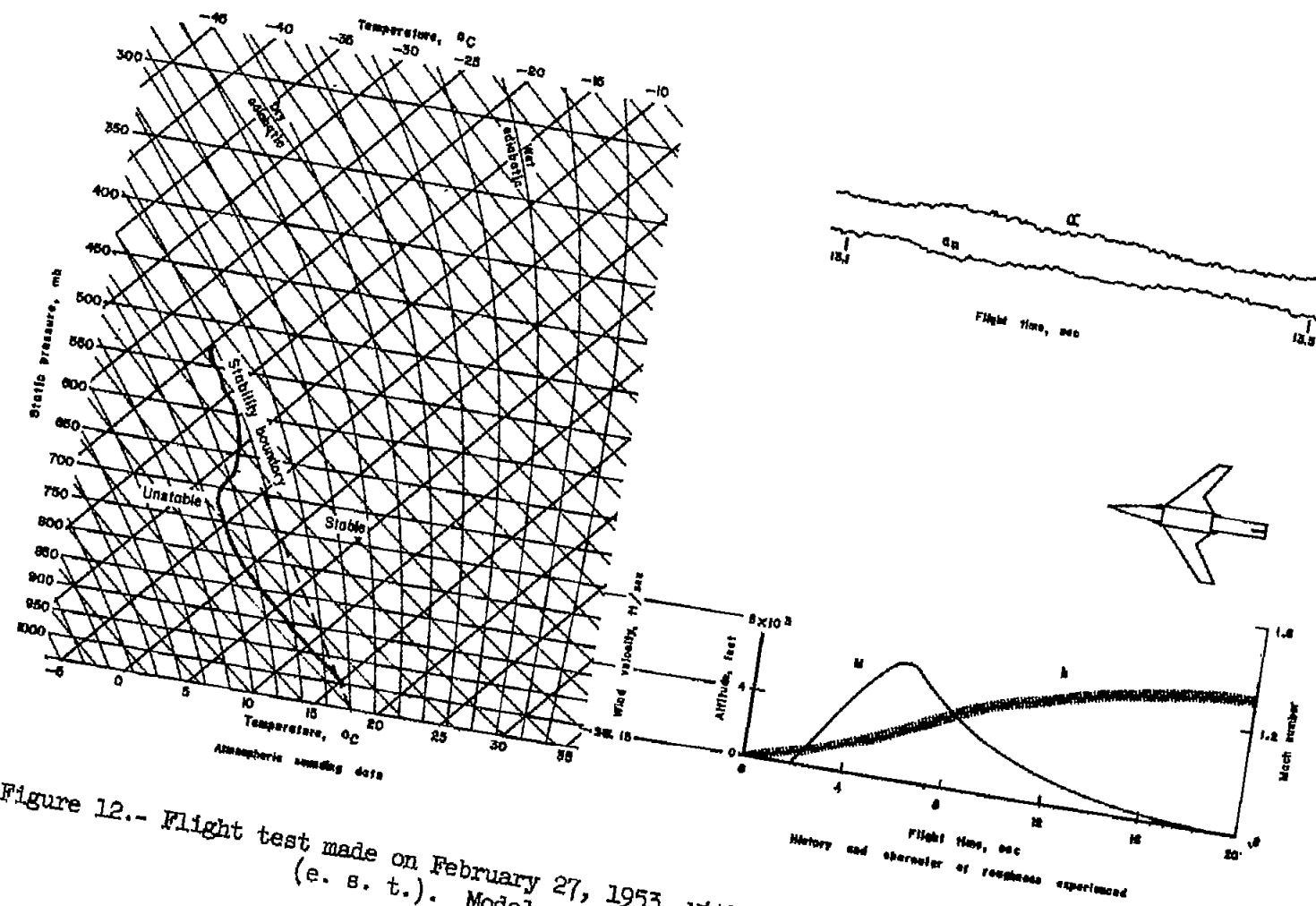


Figure 12.- Flight test made on February 27, 1953, with rawinsonde released at 2:38 p. m. (e. s. t.). Model wing loading, 28 lb/sq ft.

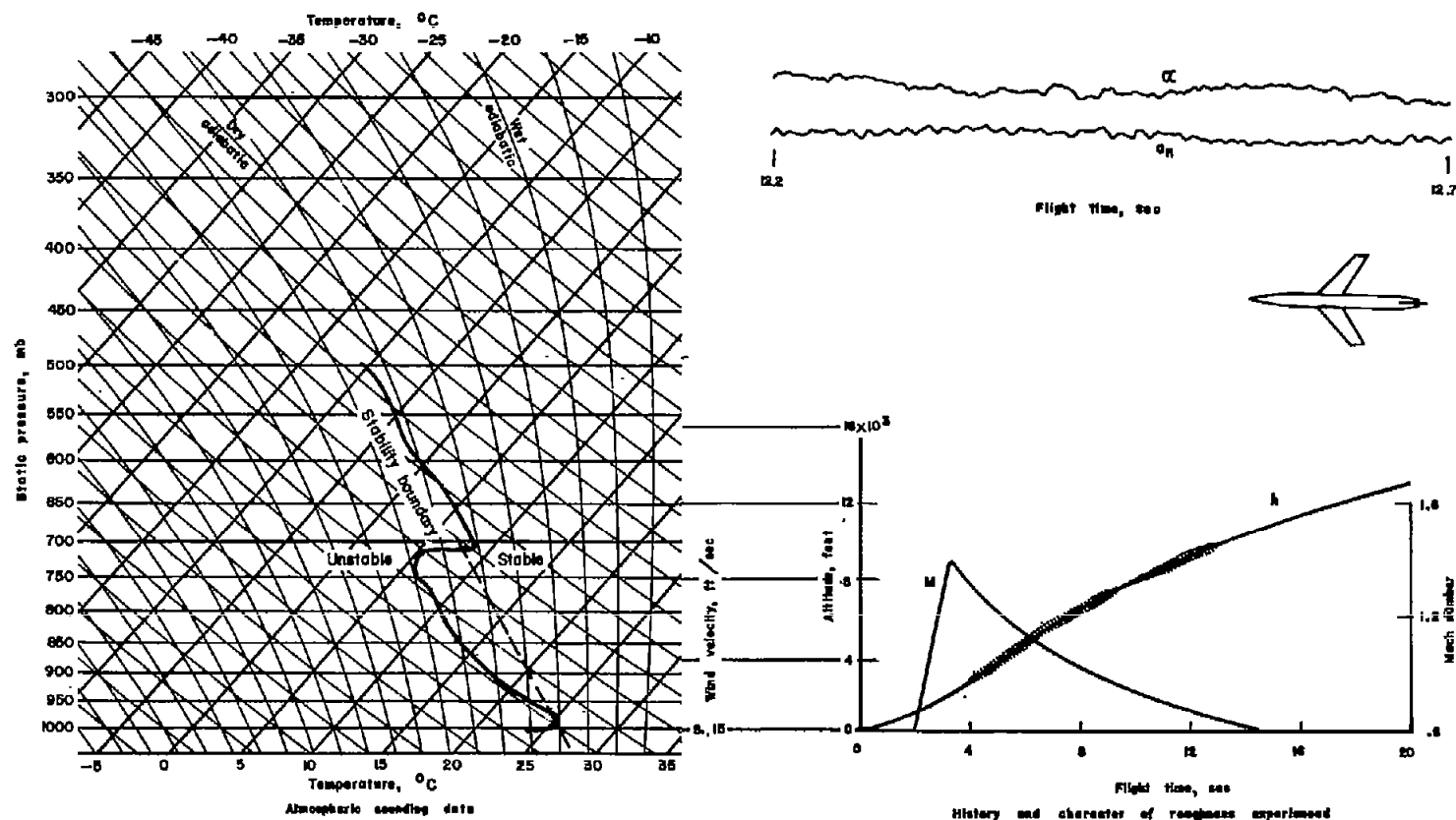


Figure 13.- Flight test made on June 4, 1954, with rawinsonde released at 12:55 p. m. (e. s. t.) and model launched at 2:31 p. m. (e. s. t.). Model wing loading, 26 lb/sq ft.

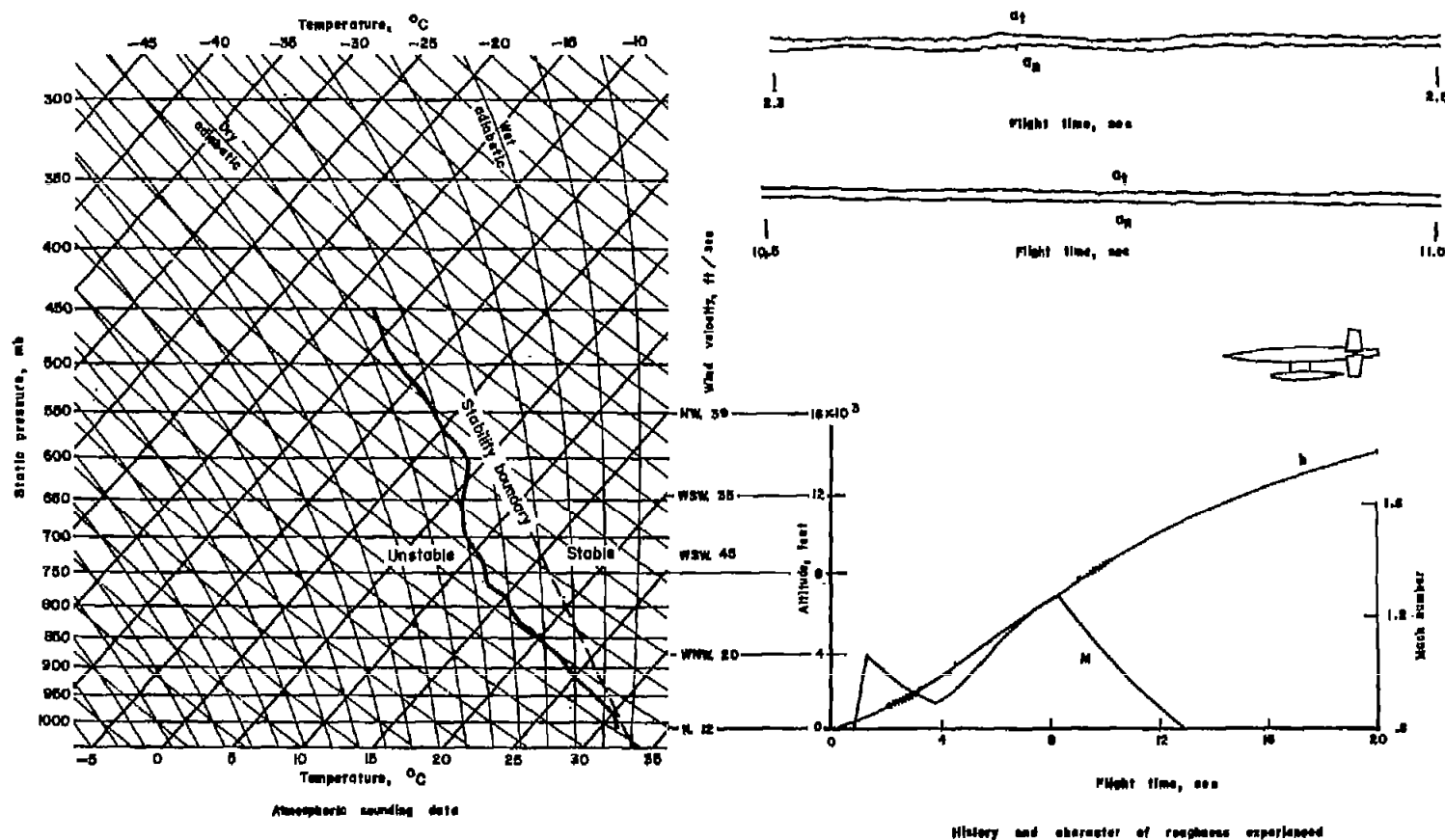


Figure 14.- Flight test made on July 30, 1953, with rawinsonde released at 3:40 p. m. (e. s. t.) and model launched at 4:17 p. m. (e. s. t.). Model wing loading, 53 lb/sq ft.

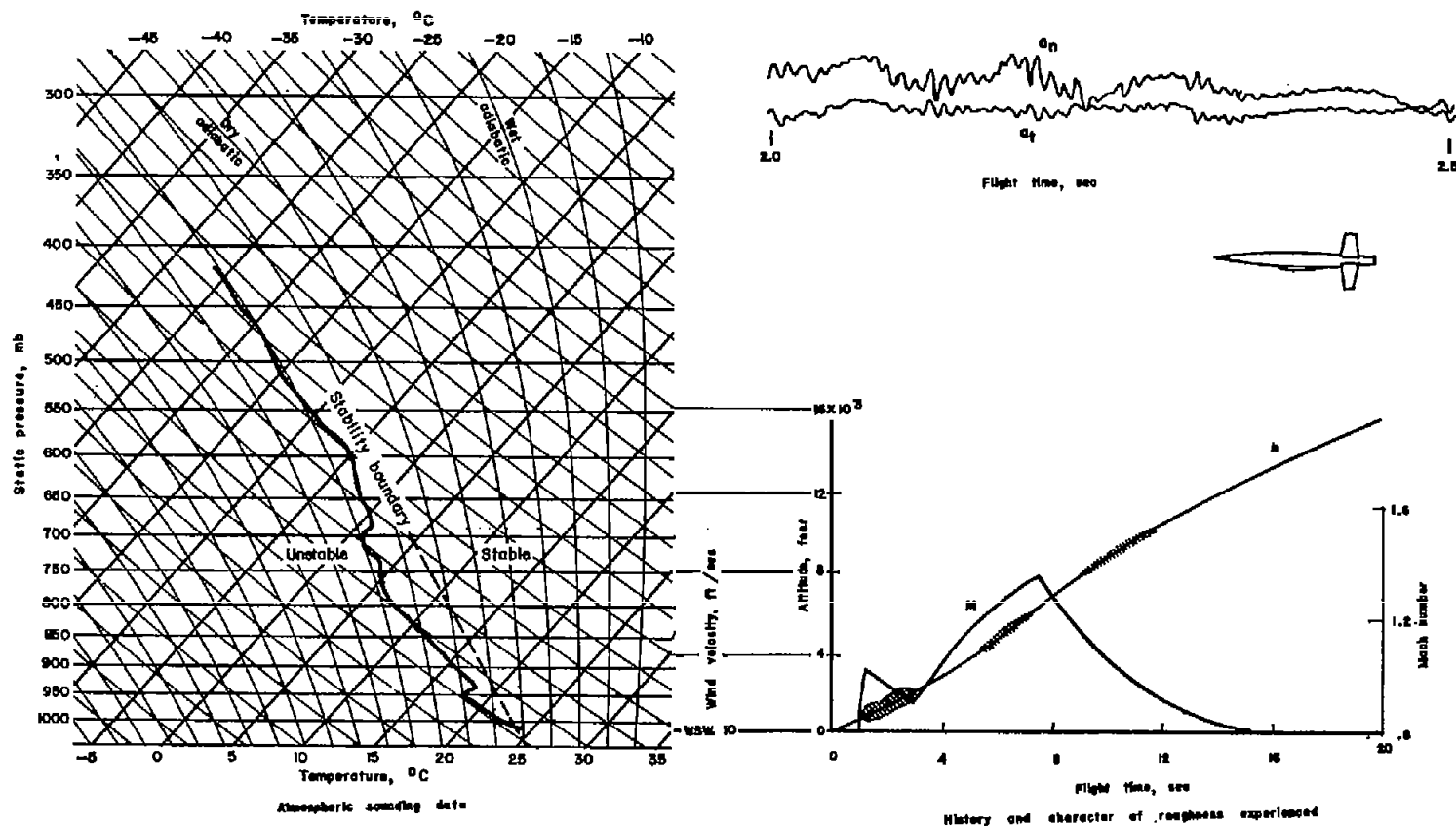


Figure 15.- Flight test made on May 6, 1952, with rawinsonde released at 4:27 p. m. (e. s. t.) and model launched at 3:23 p. m. (e. s. t.). Model wing loading, 50 lb/sq ft.

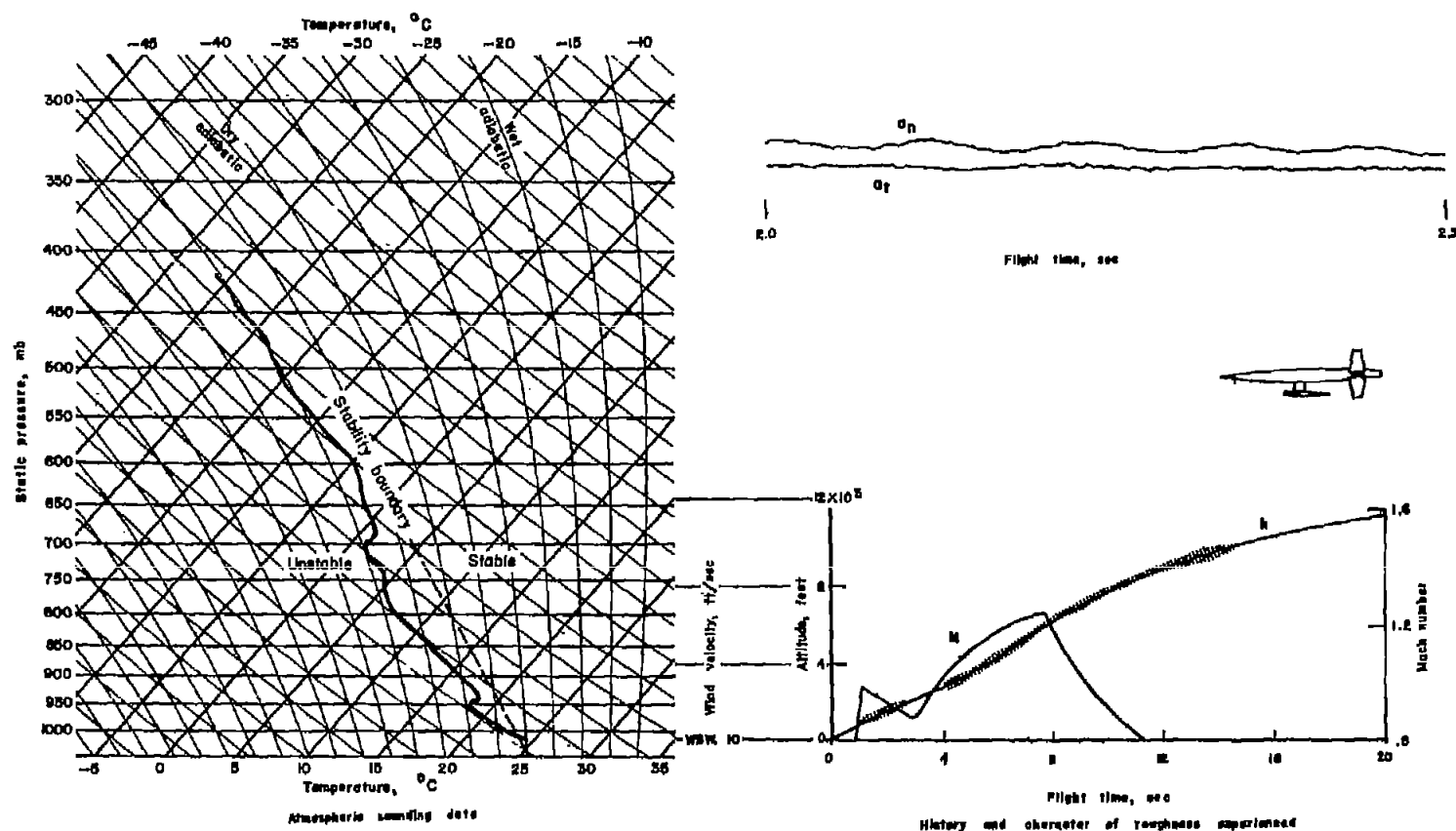


Figure 16.- Flight test made on May 6, 1952, with rawinsonde released at 4:27 p. m. (e. s. t.) and model launched at 5:12 p. m. (e. s. t.). Model wing loading, 50 lb/sq ft.

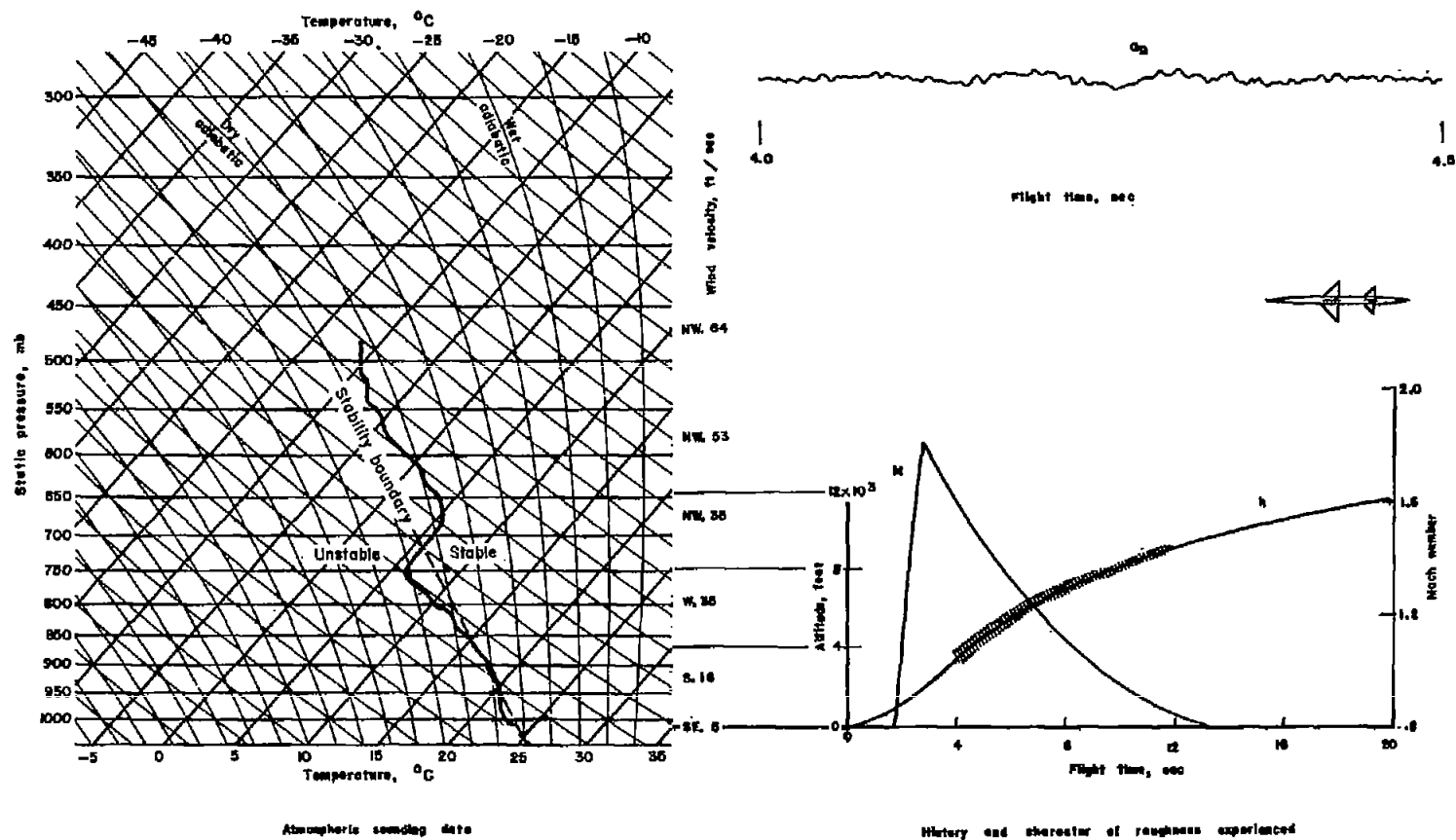


Figure 17.- Flight test made on June 30, 1954, with rawinsonde released at 2:32 p. m. (e. s. t.).
Model wing loading, 40 lb/sq ft.

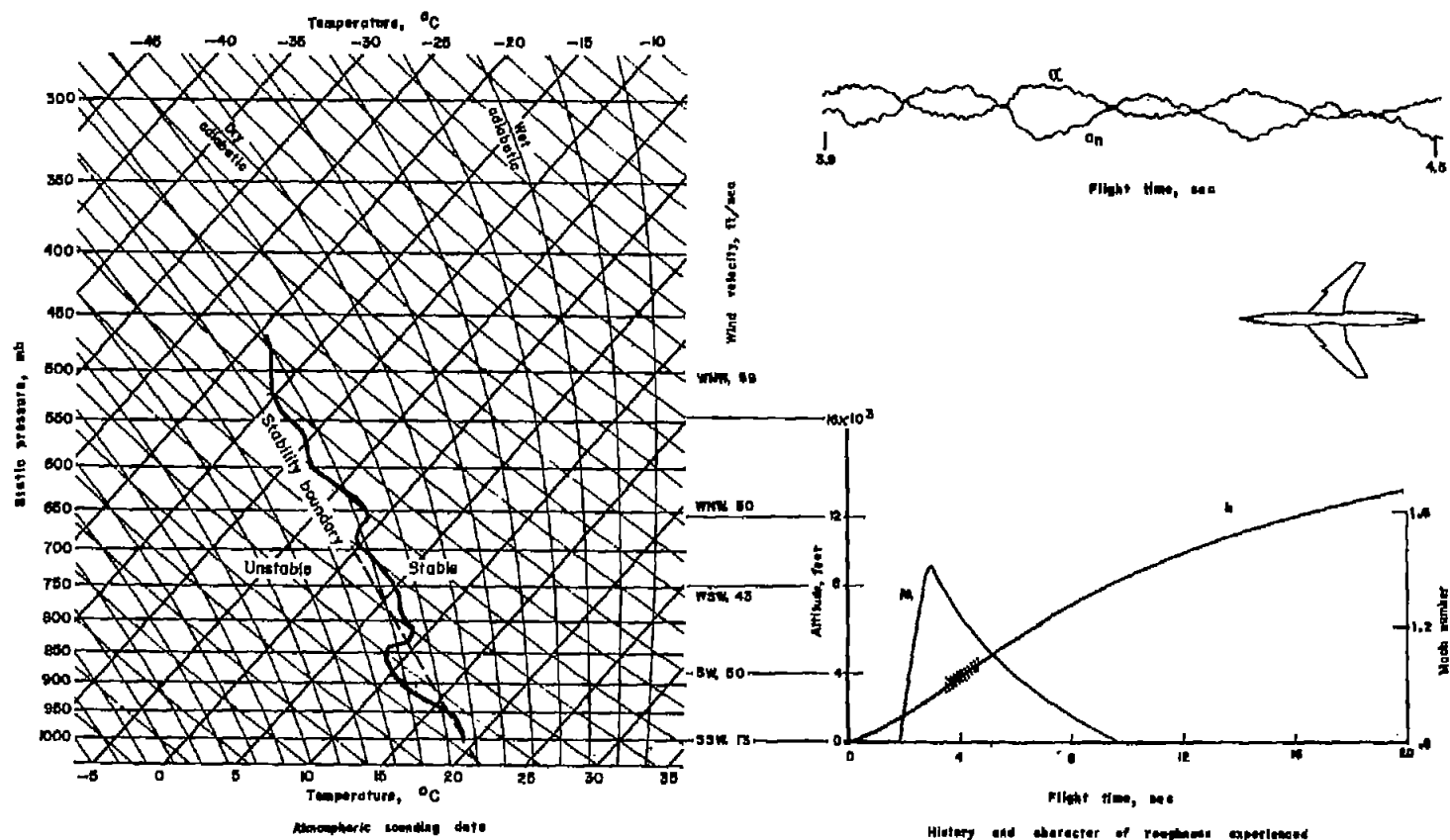


Figure 18.- Flight test made on April 14, 1954, with rawinsonde released at 2:53 p. m. (e. s. t.).
Model wing loading, 33 lb/sq ft.

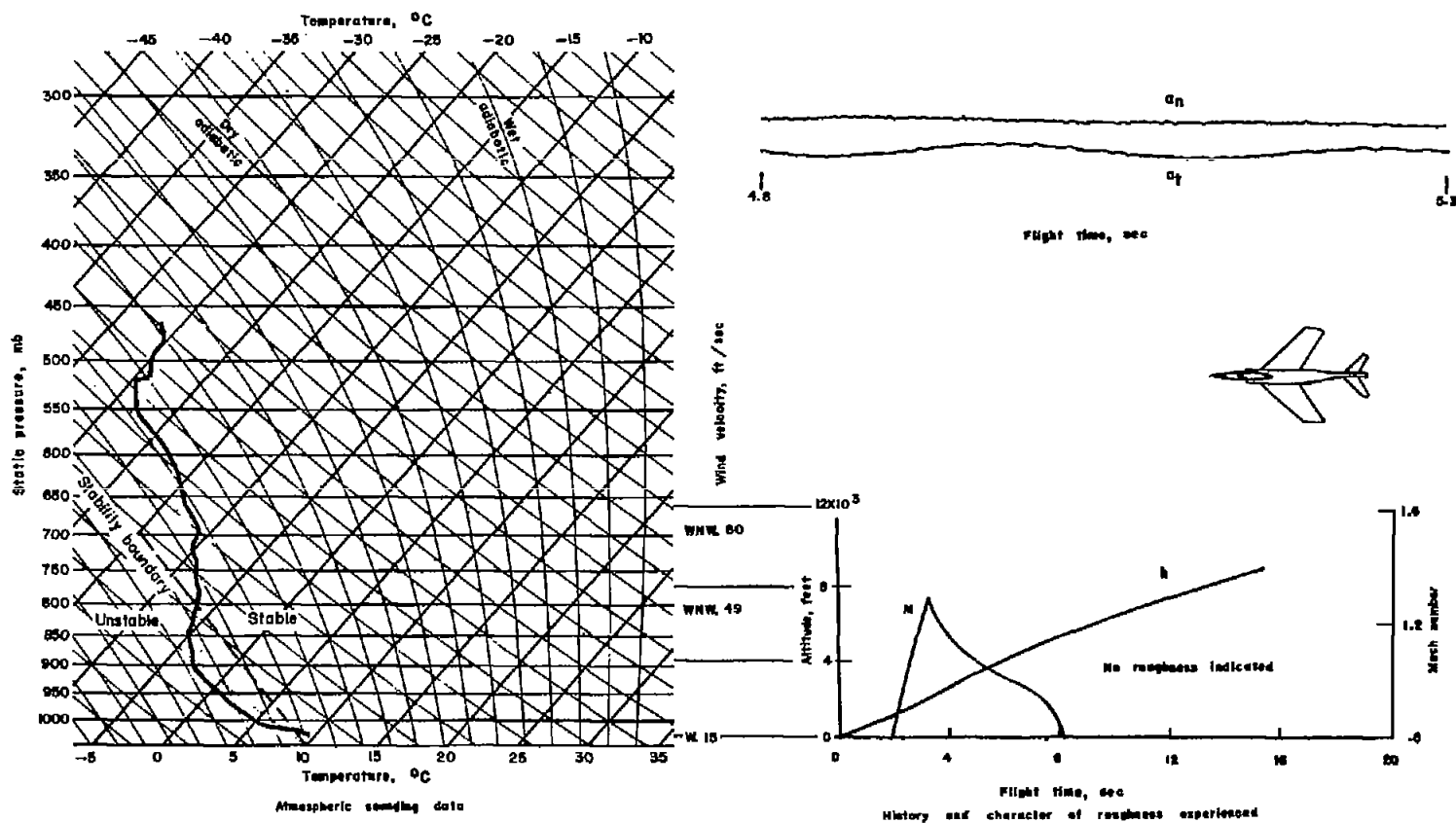


Figure 19.- Flight test made on January 26, 1955, with rawinsonde released at 2:52 p. m. (e. s. t.).
 Model wing loading, 27 lb/sq ft.

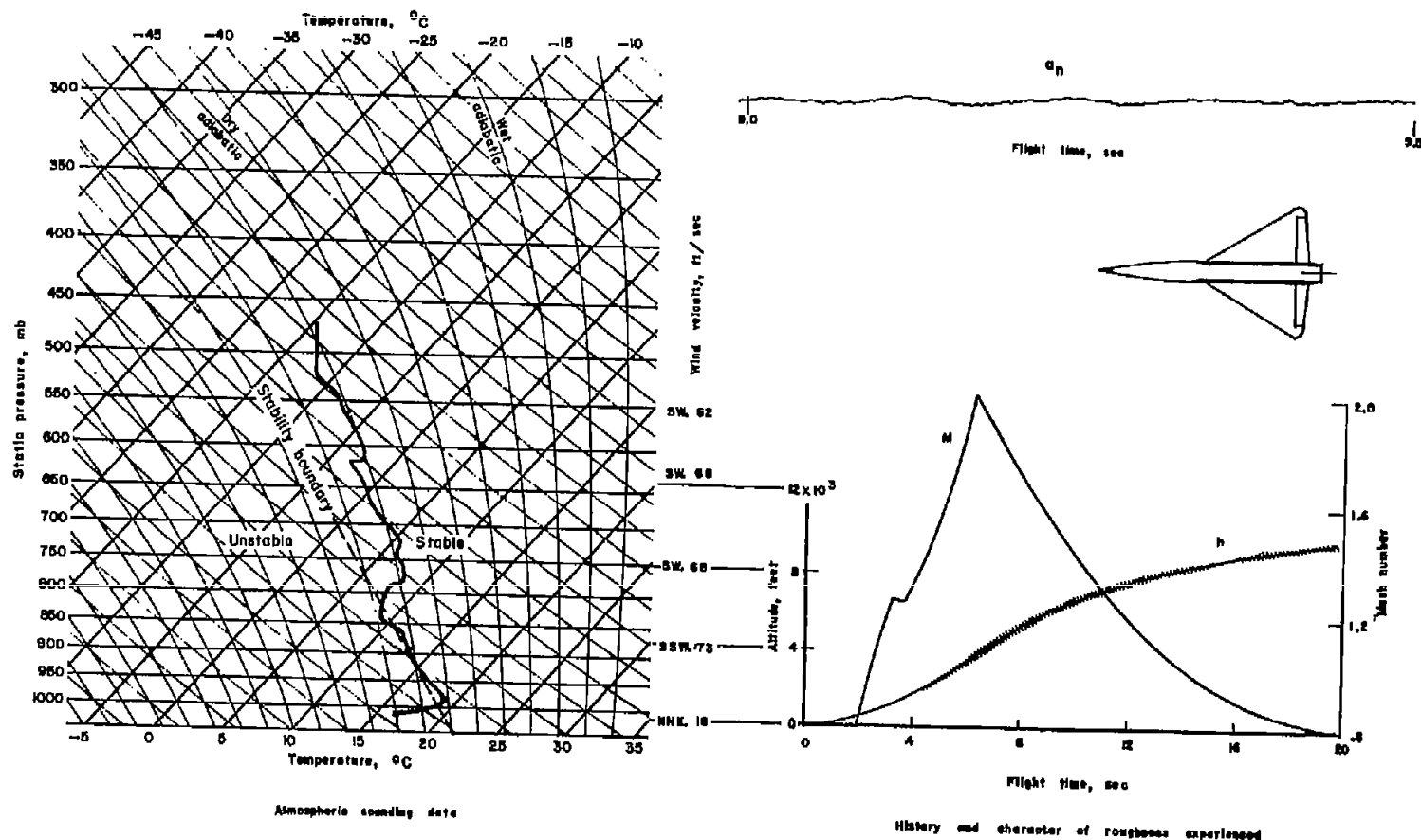


Figure 20.- Flight test made on April 14, 1955, with rawinsonde released at 2:41 p. m. (e. s. t.) and model launched at 2:29 p. m. (e. s. t.). Model wing loading, 18 lb/sq ft.

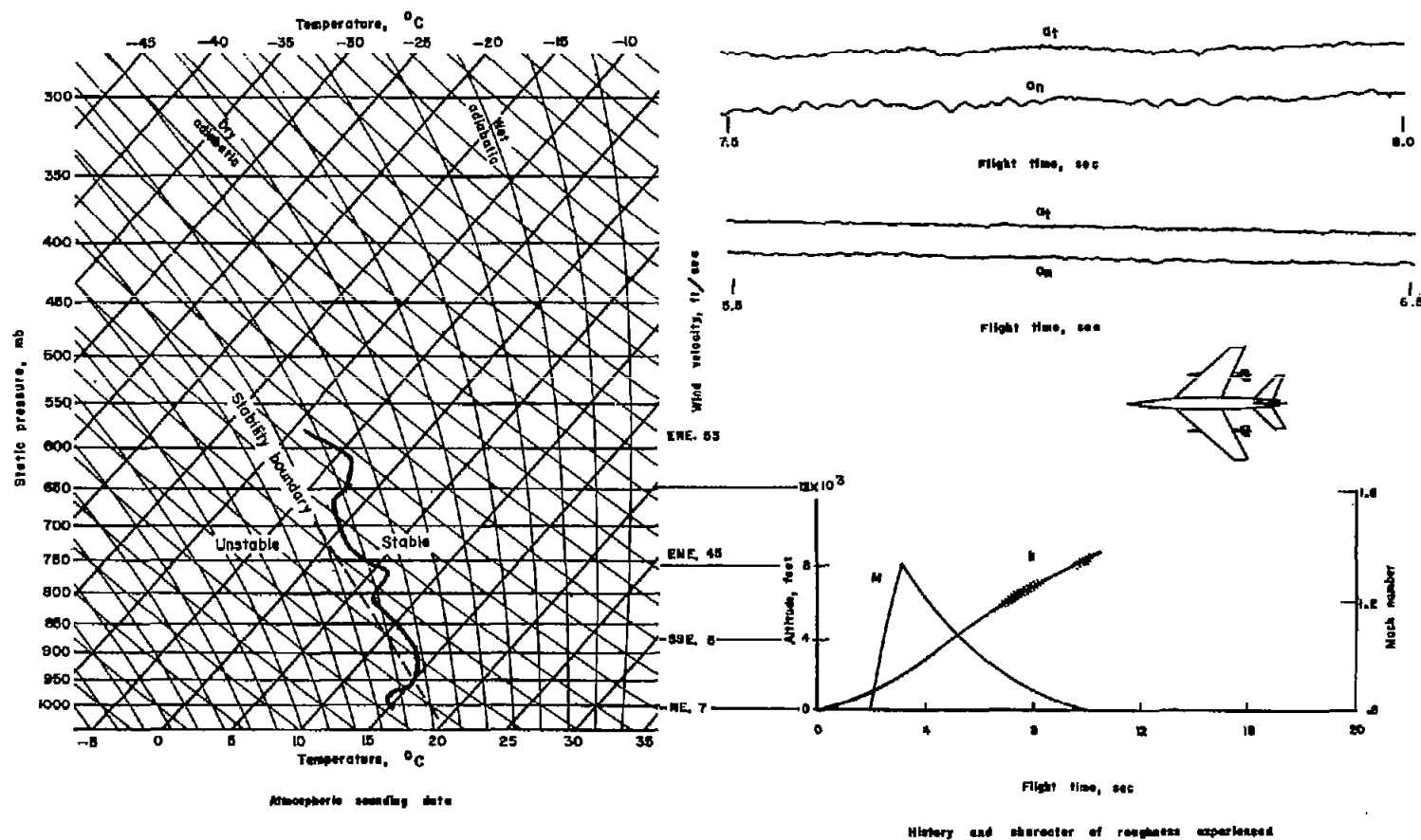


Figure 21.- Flight test made on May 18, 1954, with rawinsonde released at 2:56 p. m. (e. s. t.) and model launched at 2:34 p. m. (e. s. t.). Model wing loading, 25 lb/sq ft.

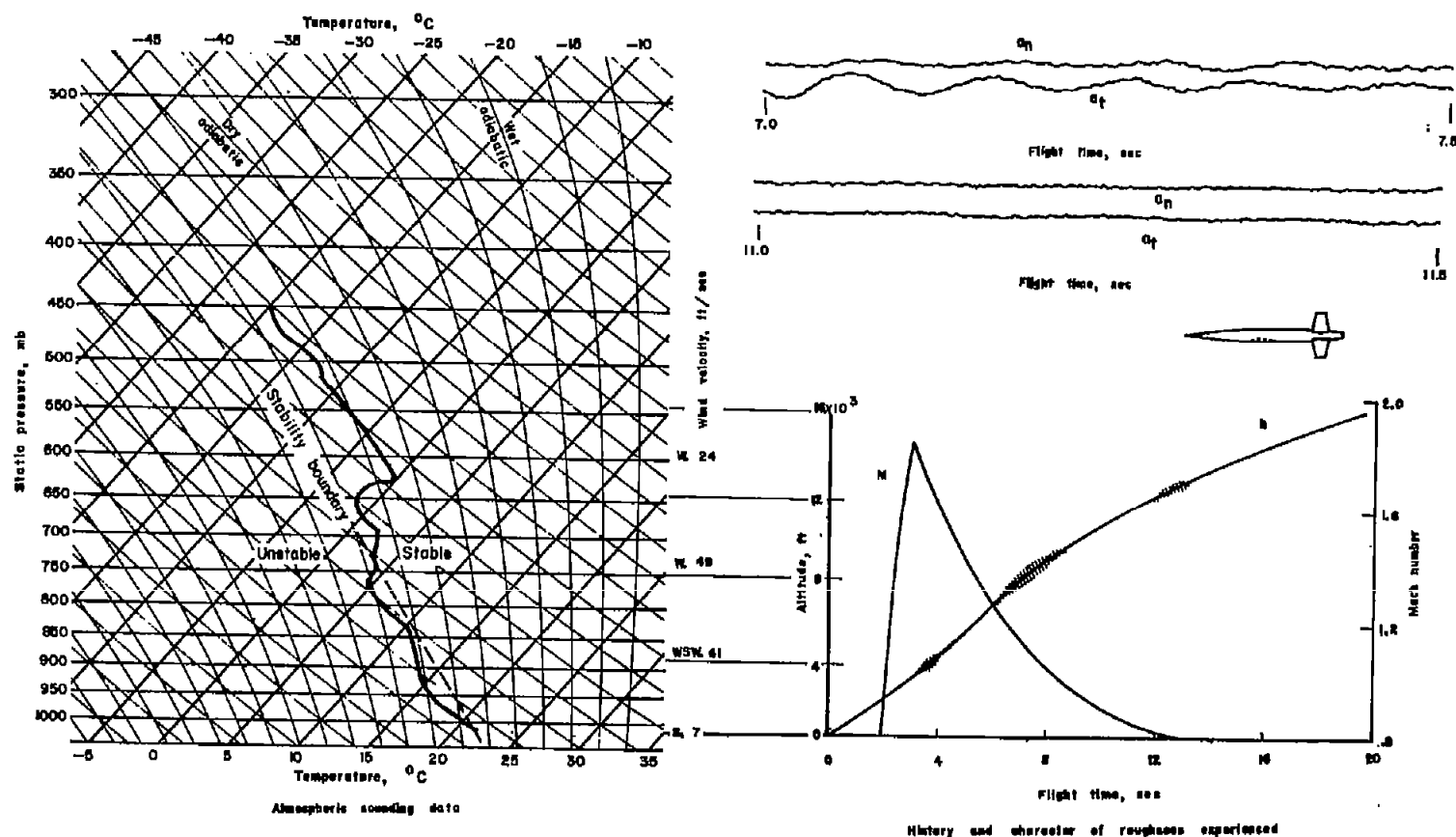


Figure 22.- Flight test made on February 15, 1954, with rawinsonde released at 2:32 p. m. (e. s. t.) and model launched at 3:00 p. m. (e. s. t.). Model wing loading, 44 lb/sq ft.

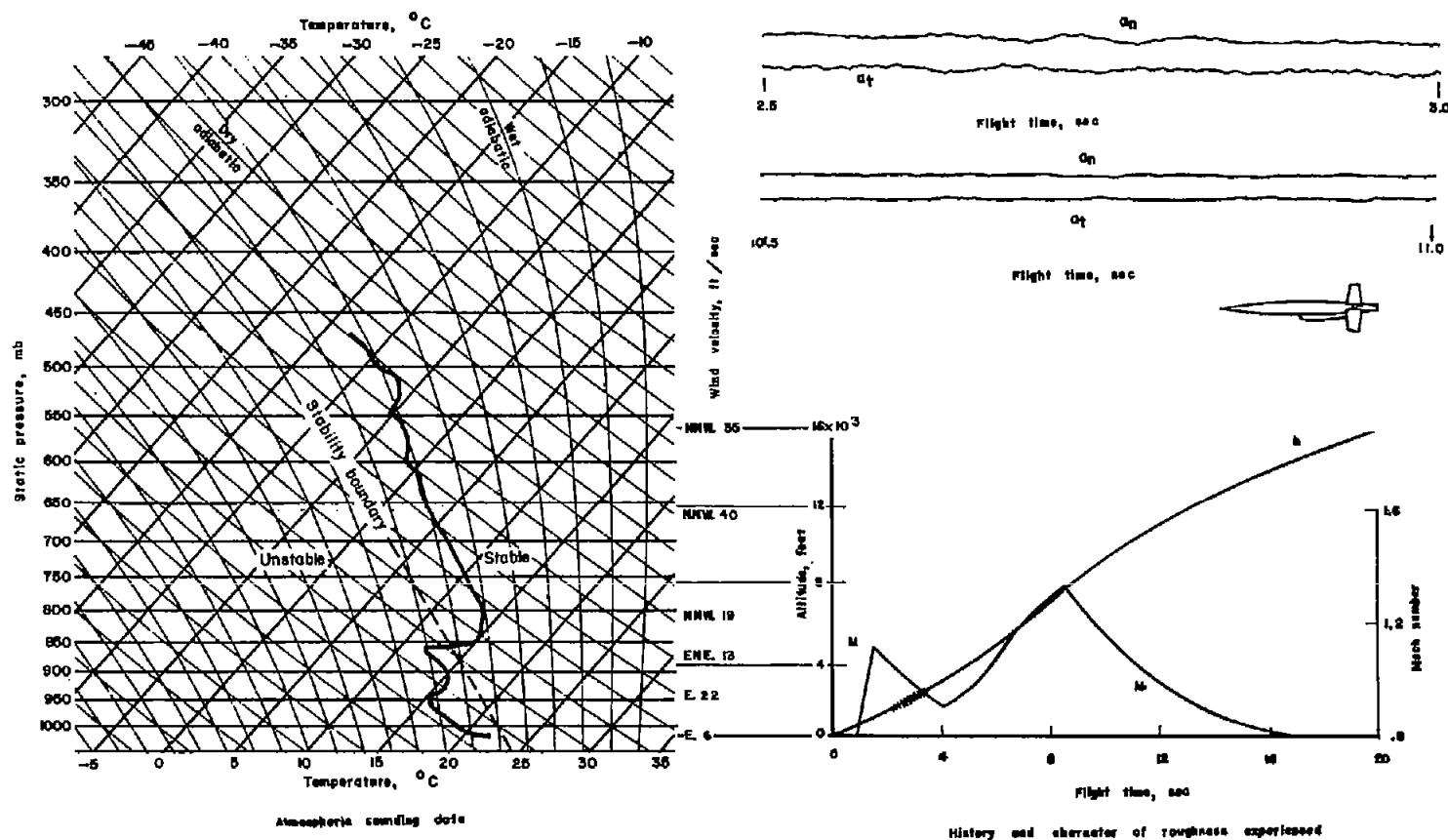
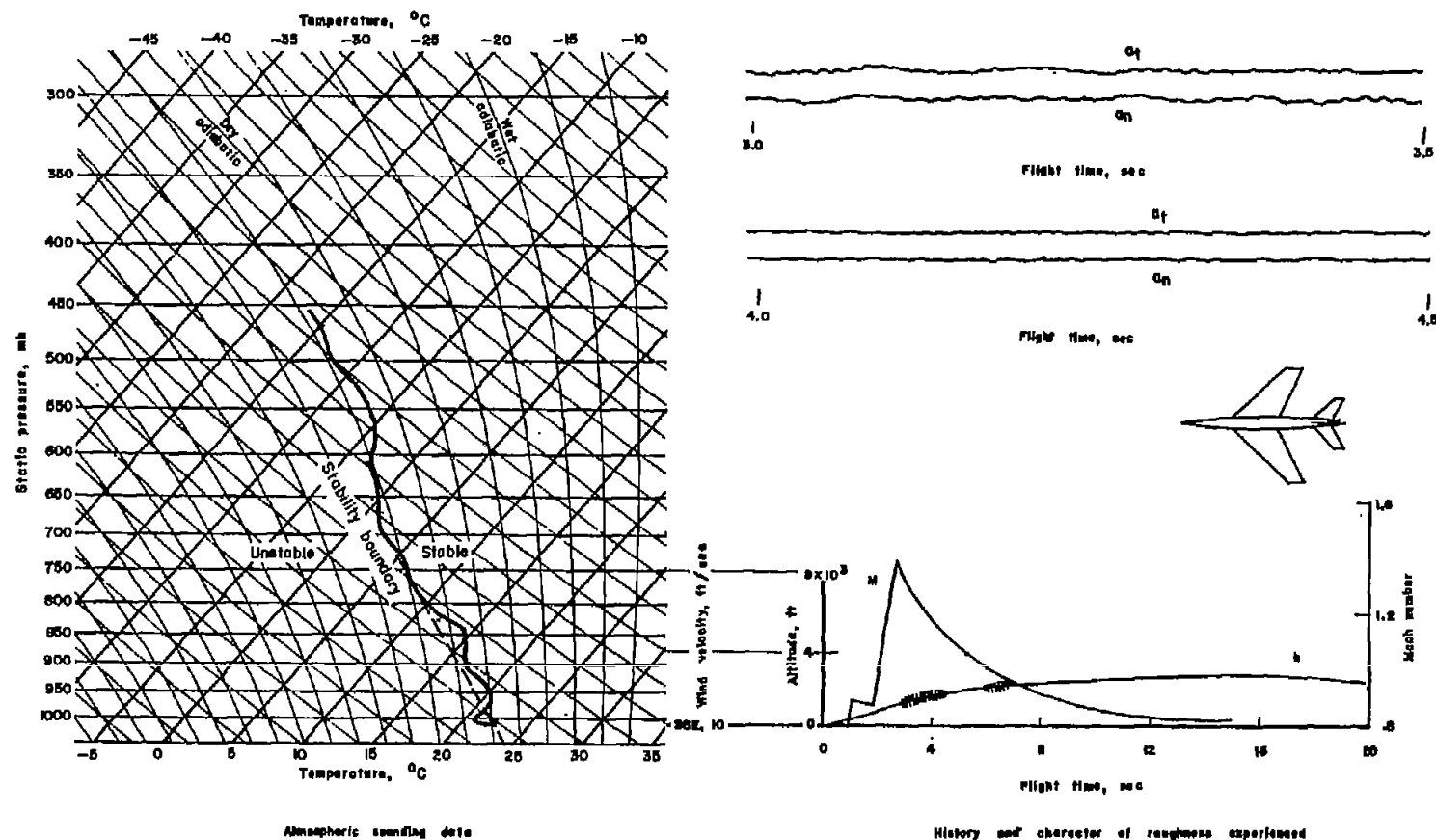


Figure 23.- Flight test made on August 3, 1953, with rawinsonde released at 4:14 p. m. (e. s. t.) and model launched at 3:42 p. m. (e. s. t.). Model wing loading, 50 lb/sq ft.



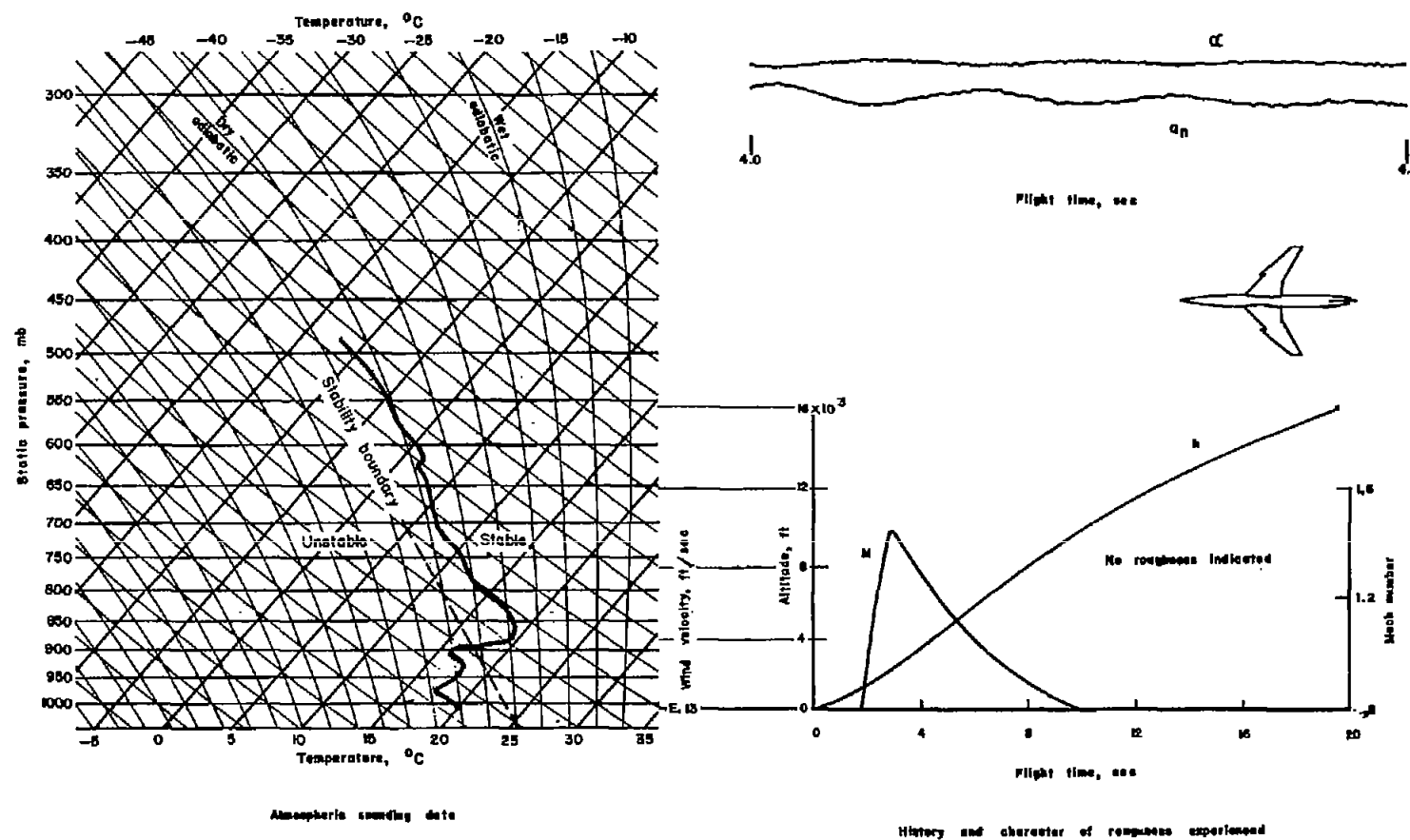


Figure 25.- Flight test made on June 24, 1955, with rawinsonde released at 4:04 p. m. (e. s. t.).
Model wing loading, 21 lb/sq ft.

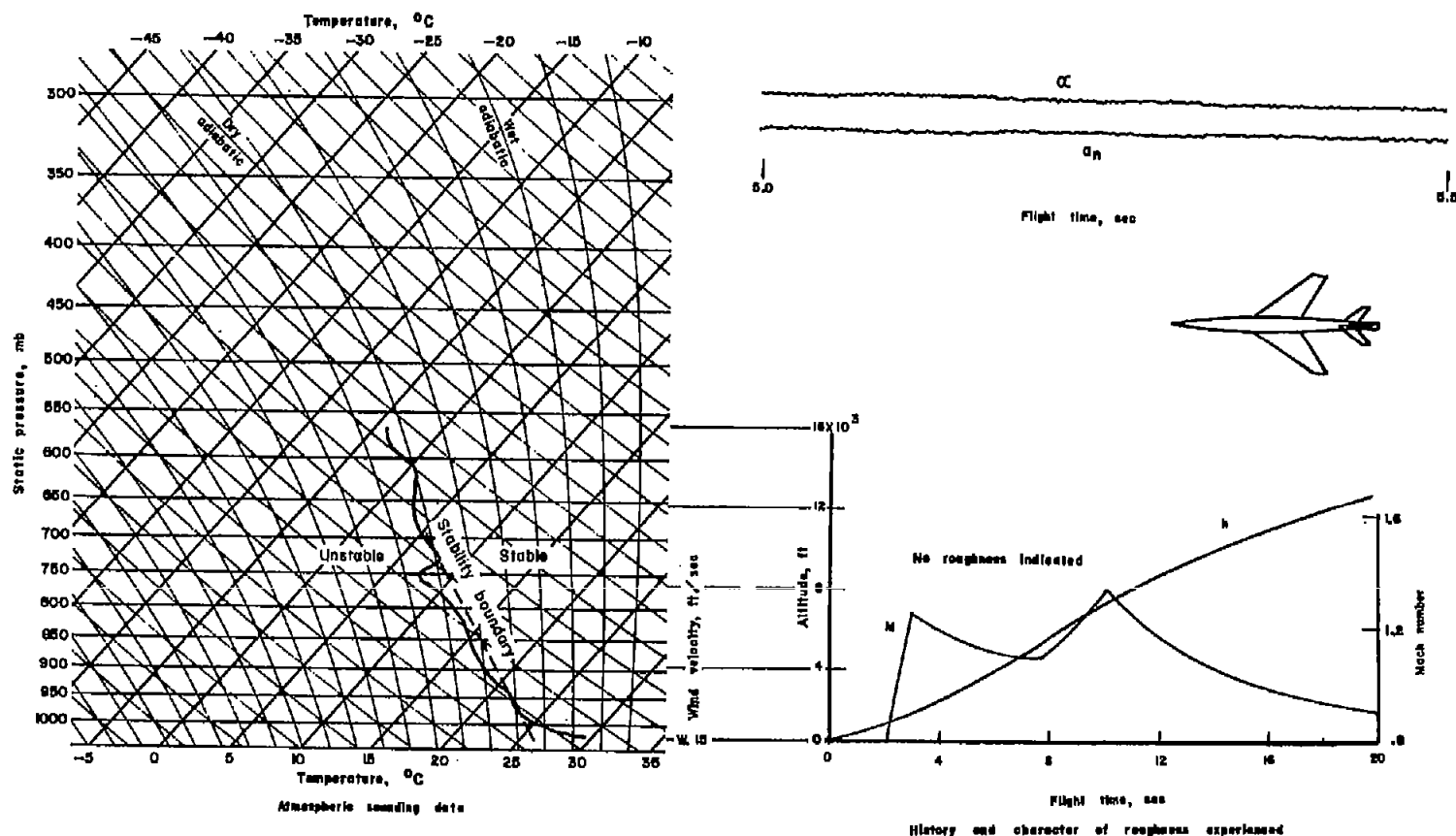


Figure 26.- Flight test made on June 24, 1955, with rawinsonde released at 1:43 p. m. (e. s. t.).
 Model wing loading, 35 lb/sq ft.

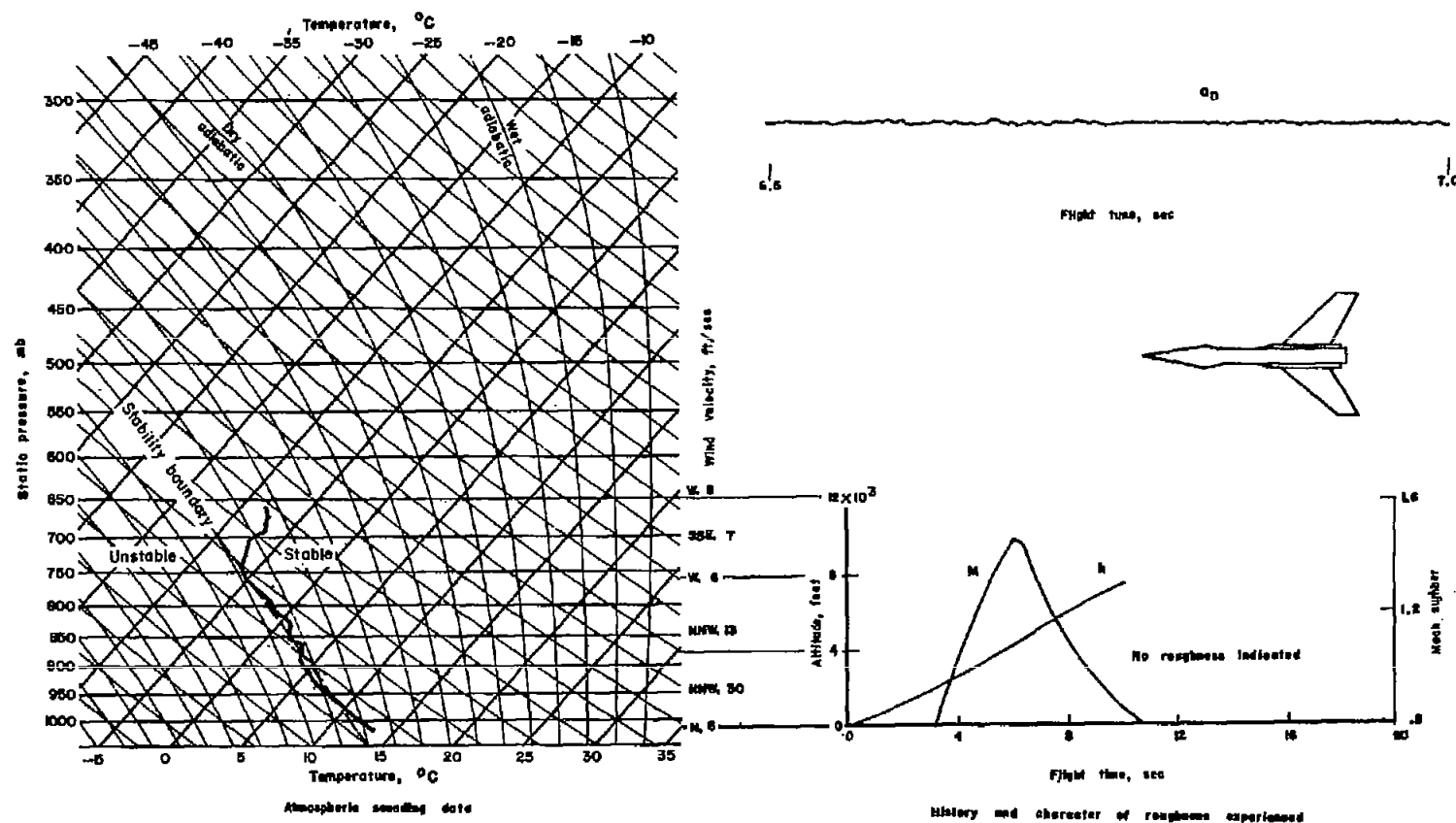


Figure 27.- Flight test made on October 20, 1954, with rawinsonde released at 5:13 p. m. (e. s. t.) and model launched at 3:58 p. m. (e. s. t.). Model wing loading, 22 lb/sq ft.

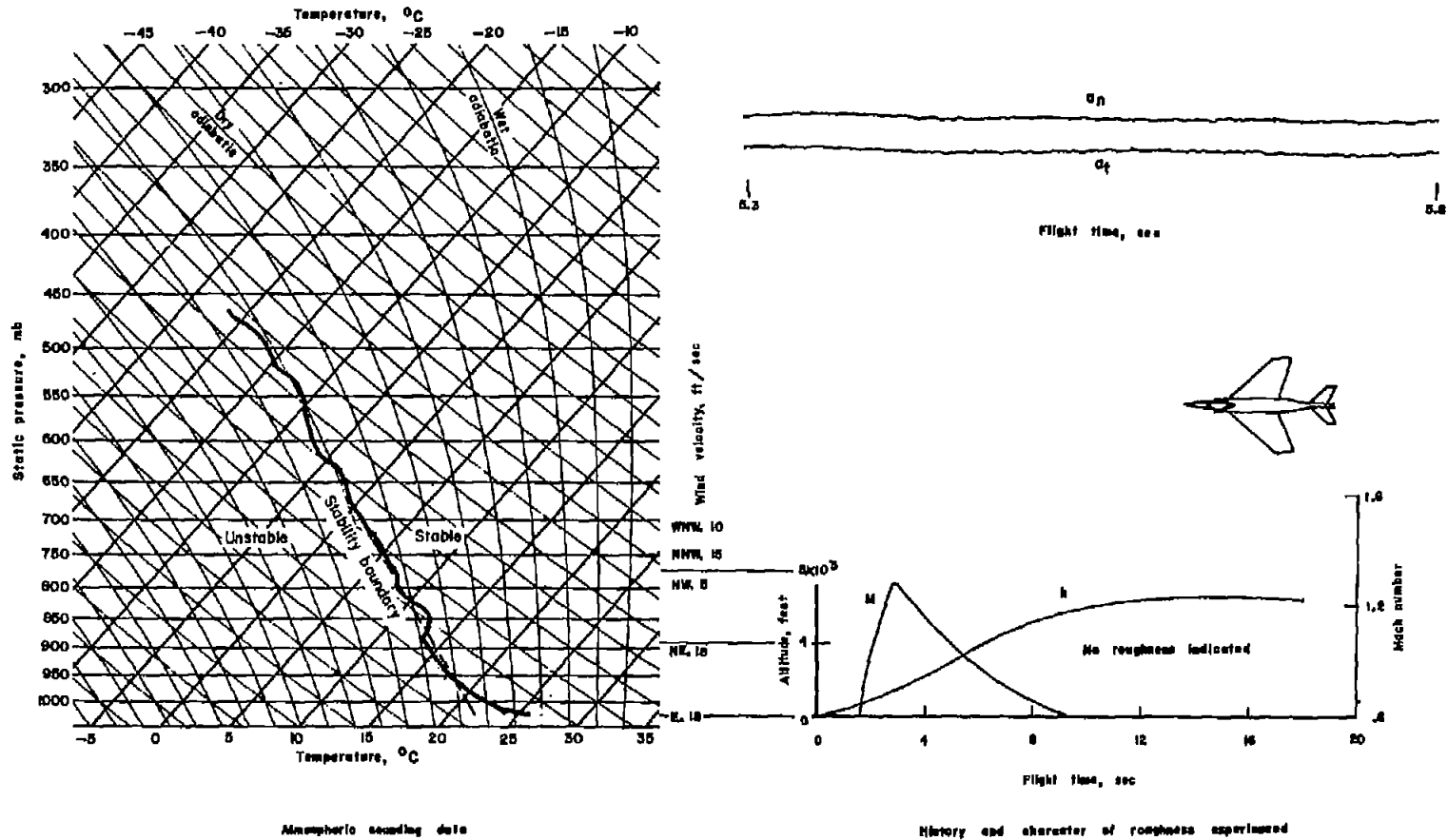


Figure 28.- Flight test made on June 15, 1955, with rawinsonde released at 3:07 p. m. (e. s. t.).
Model wing loading, 27 lb/sq ft.

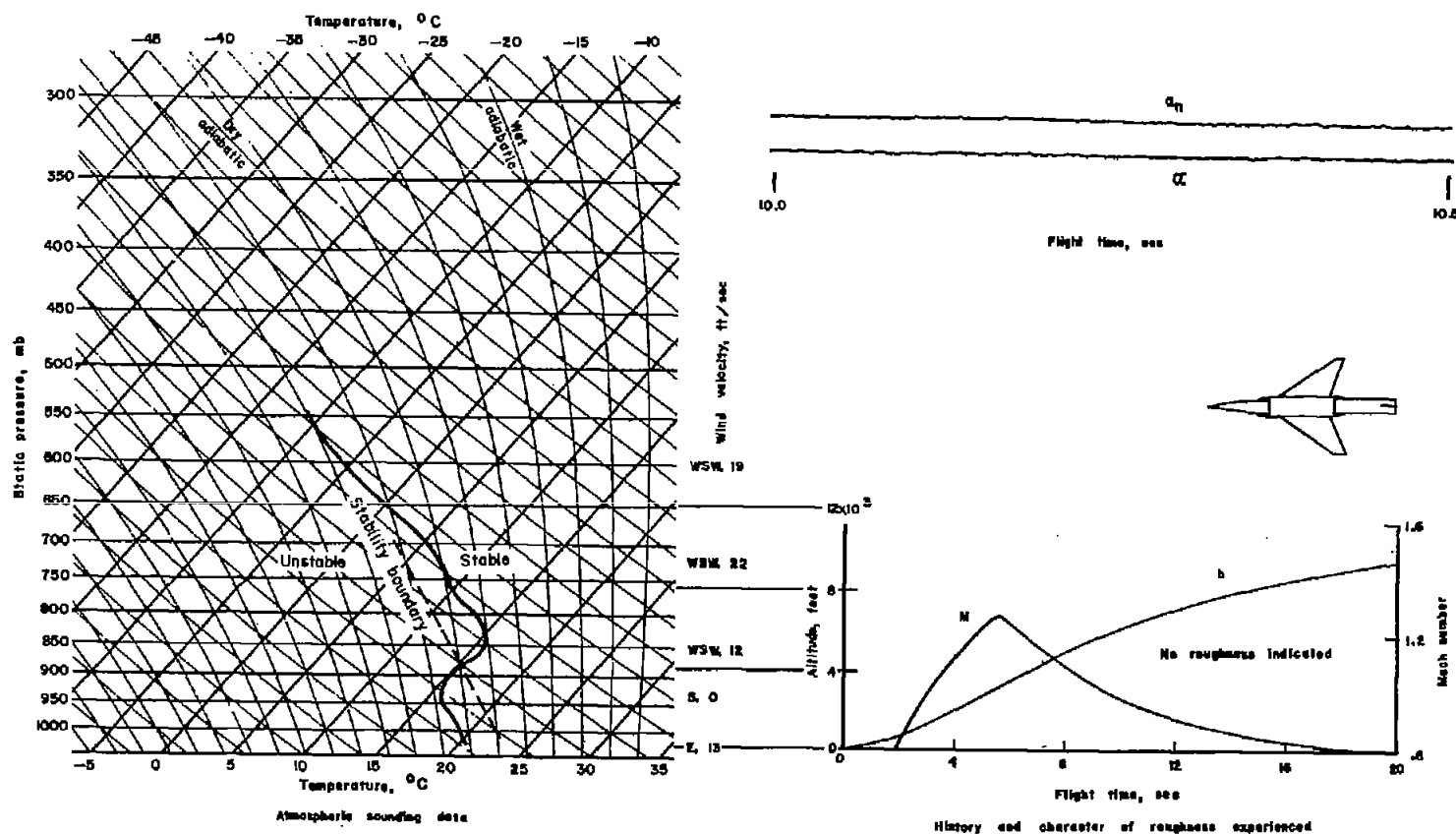


Figure 29.- Flight test made on November 1, 1953, with rawinsonde released at 3:10 p. m. (e. s. t.).
Model wing loading, 28 lb/sq ft.

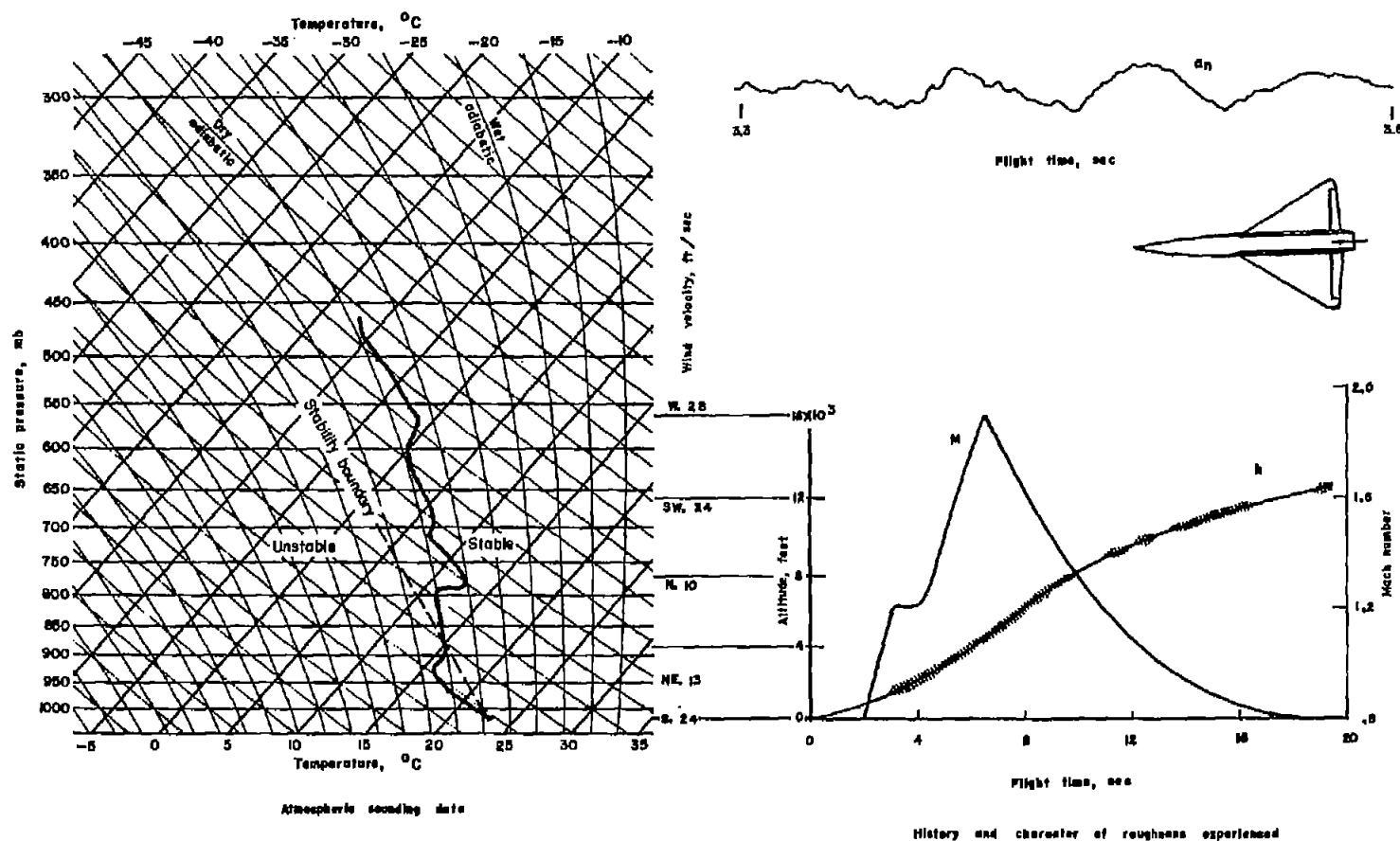


Figure 30.- Flight test made on August 25, 1955, with rawinsonde released at 3:48 p. m. (e. s. t.) and model launched at 2:12 p. m. (e. s. t.). Model wing loading, 18 lb/sq ft.

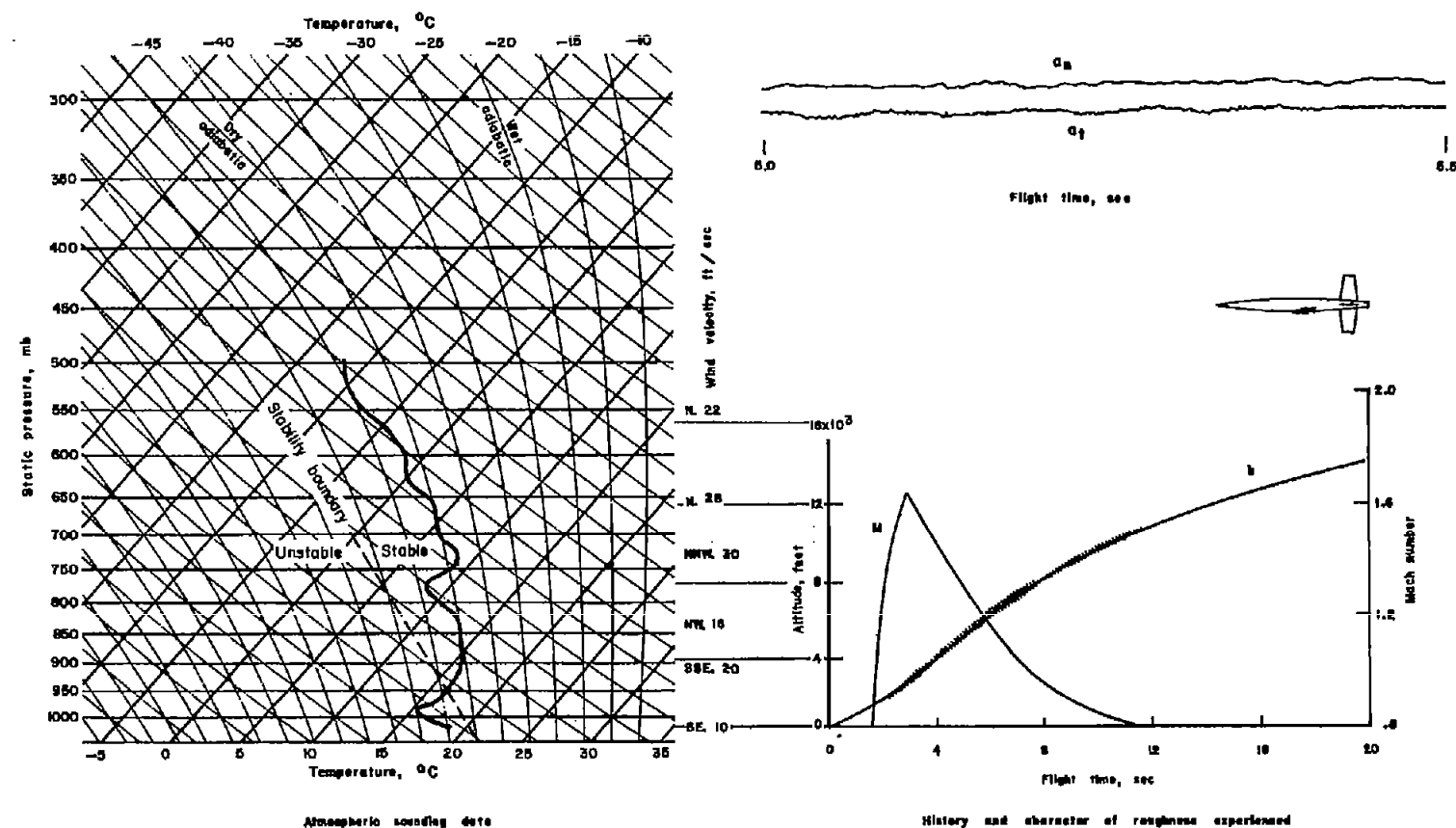


Figure 31.- Flight test made on June 9, 1954, with rawinsonde released at 2:36 p. m. (e. s. t.) and model launched at 2:08 p. m. (e. s. t.). Model wing loading, 49 lb/sq ft.

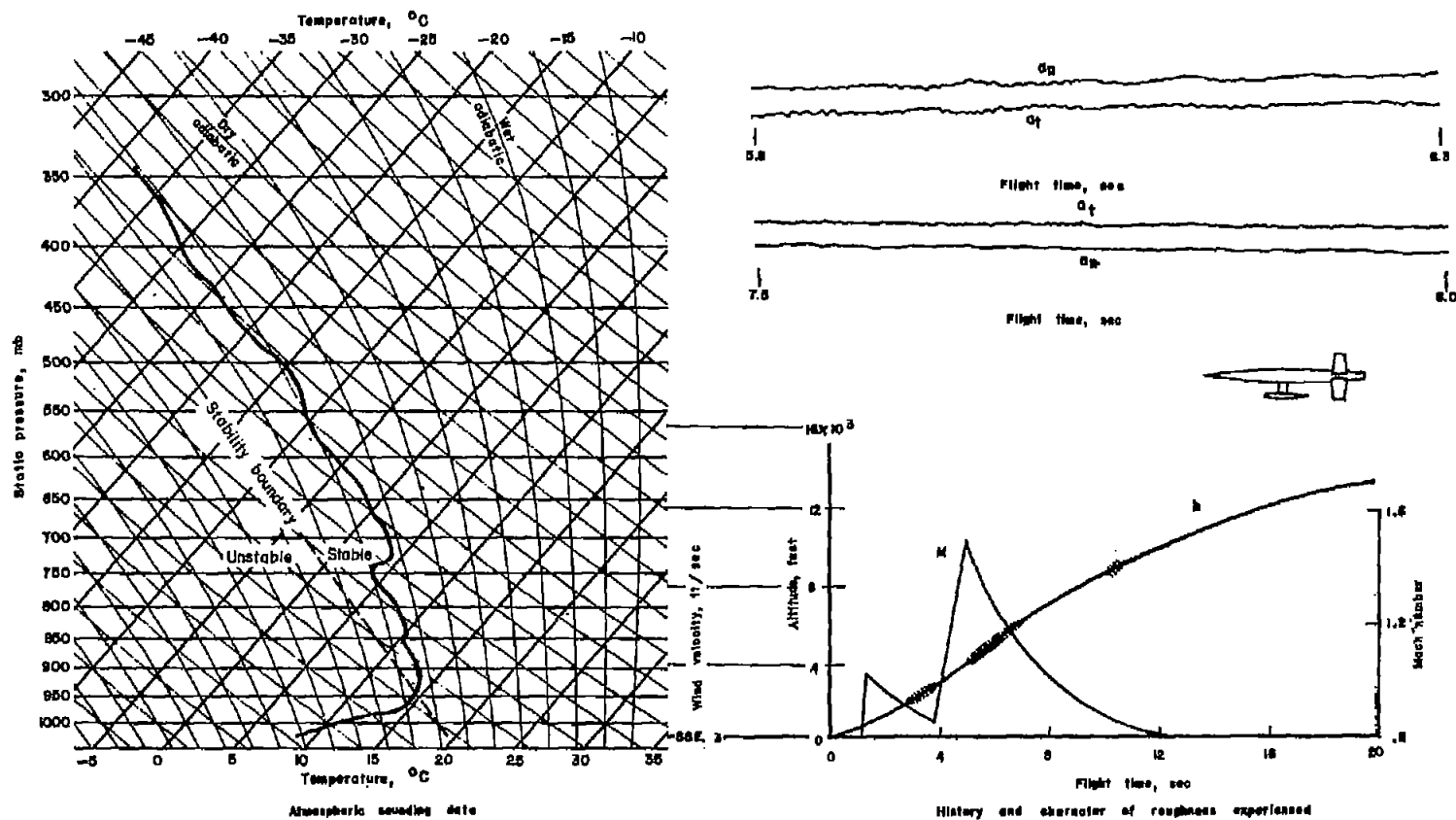


Figure 32.- Flight test made on January 14, 1953, with rawinsonde released at 3:17 p. m. (e. s. t.) and model launched at 3:57 p. m. (e. s. t.). Model wing loading, 50 lb/sq ft.

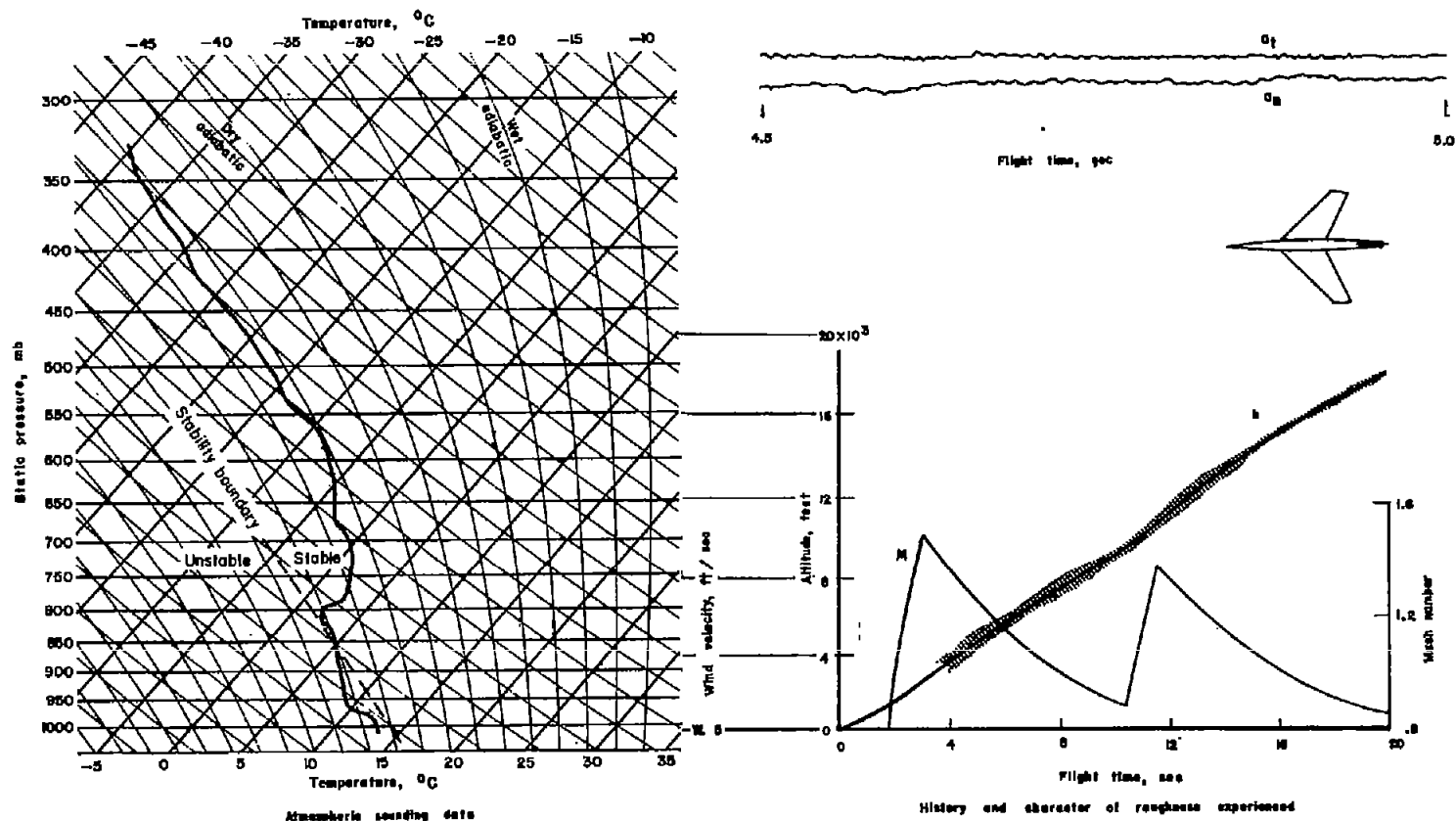


Figure 33.- Flight test made on December 18, 1952, with rawinsonde released at 2:58 p. m. (e. s. t.) and model launched at 3:43 p. m. (e. s. t.). Model wing loading, 22 lb/sq ft.

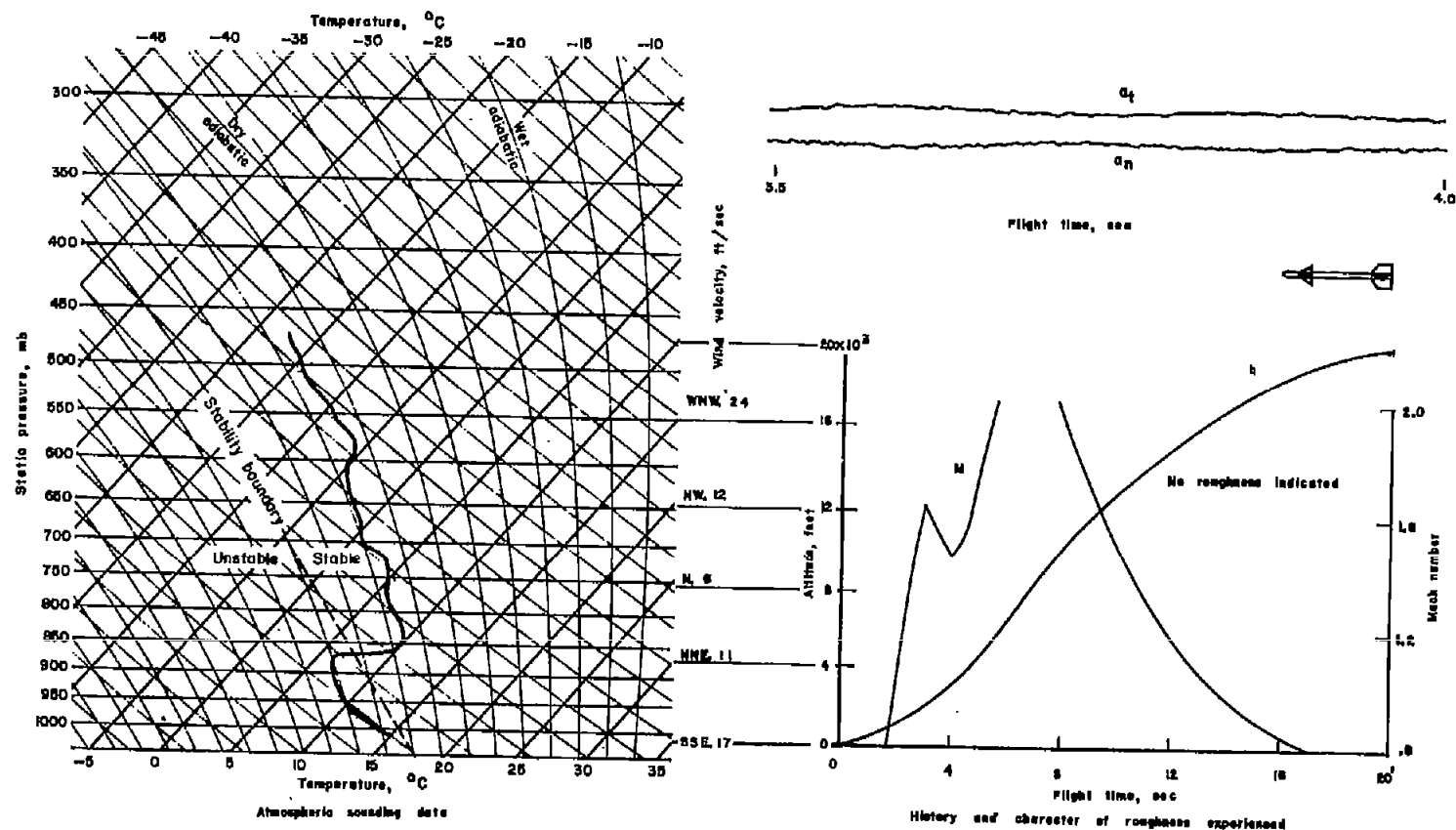


Figure 34.- Flight test made on October 13, 1953, with rawinsonde released at 4:02 p. m. (e. s. t.).
Model wing loading, 53 lb/sq ft.

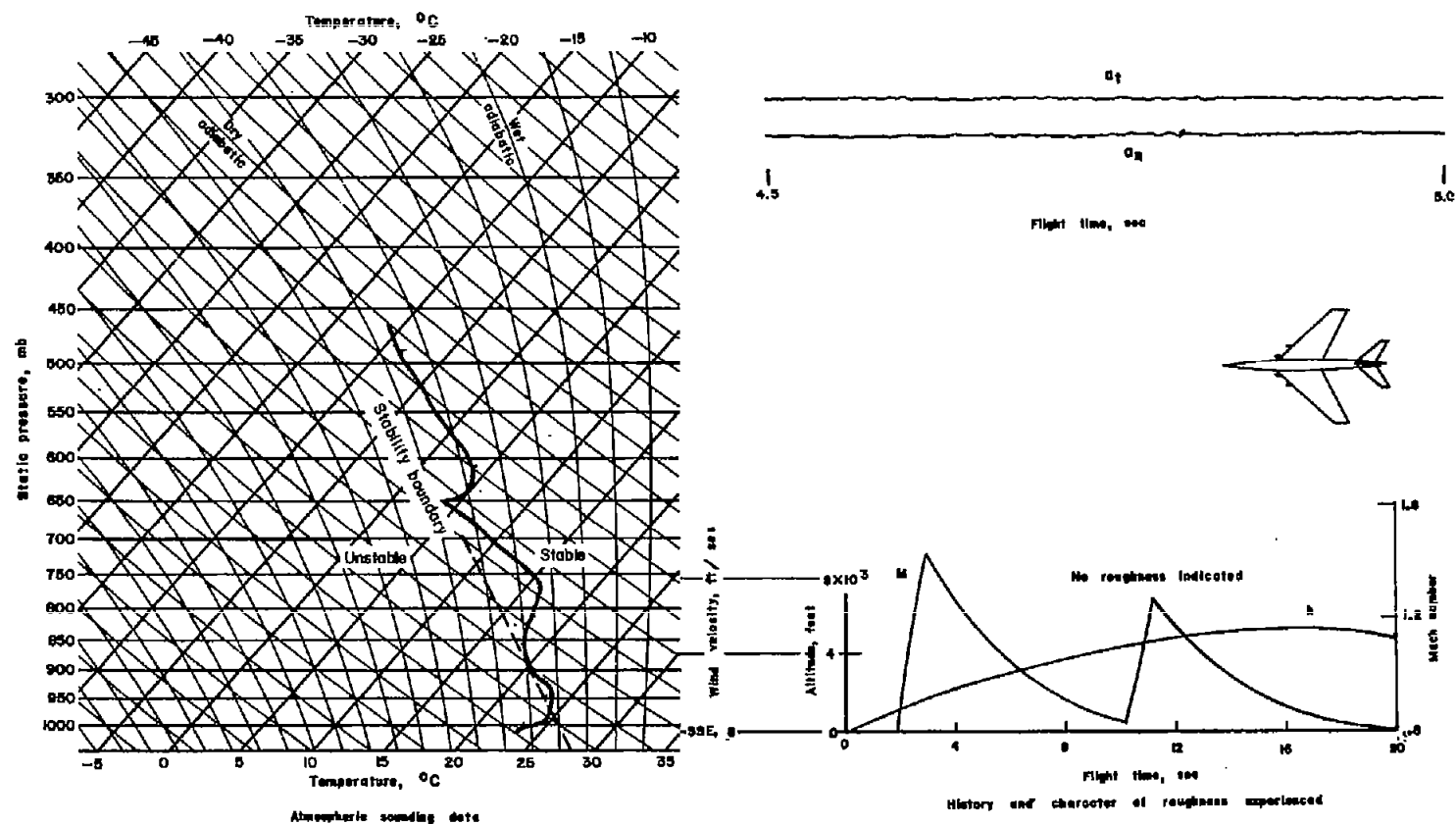


Figure 35.- Flight test made on April 30, 1953, with rawinsonde released at 2:33 p. m. (e. s. t.) and model launched at 1:53 p. m. (e. s. t.). Model wing loading, 24 lb/sq ft.

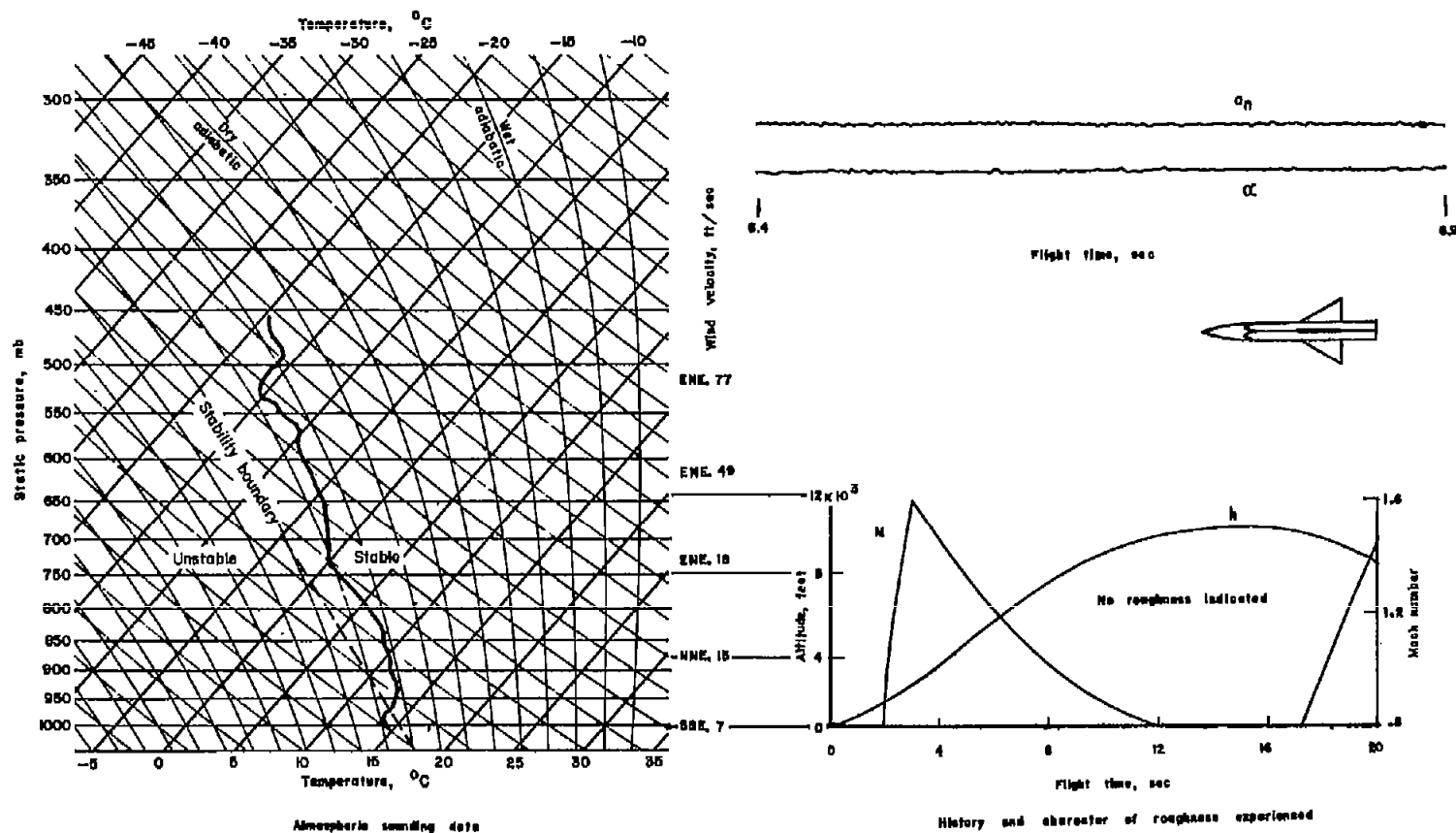


Figure 36.- Flight test made on May 19, 1954, with rawinsonde released at 2:06 p. m. (e. s. t.) and model launched at 2:15 p. m. (e. s. t.). Model wing loading, 43 lb/sq ft.

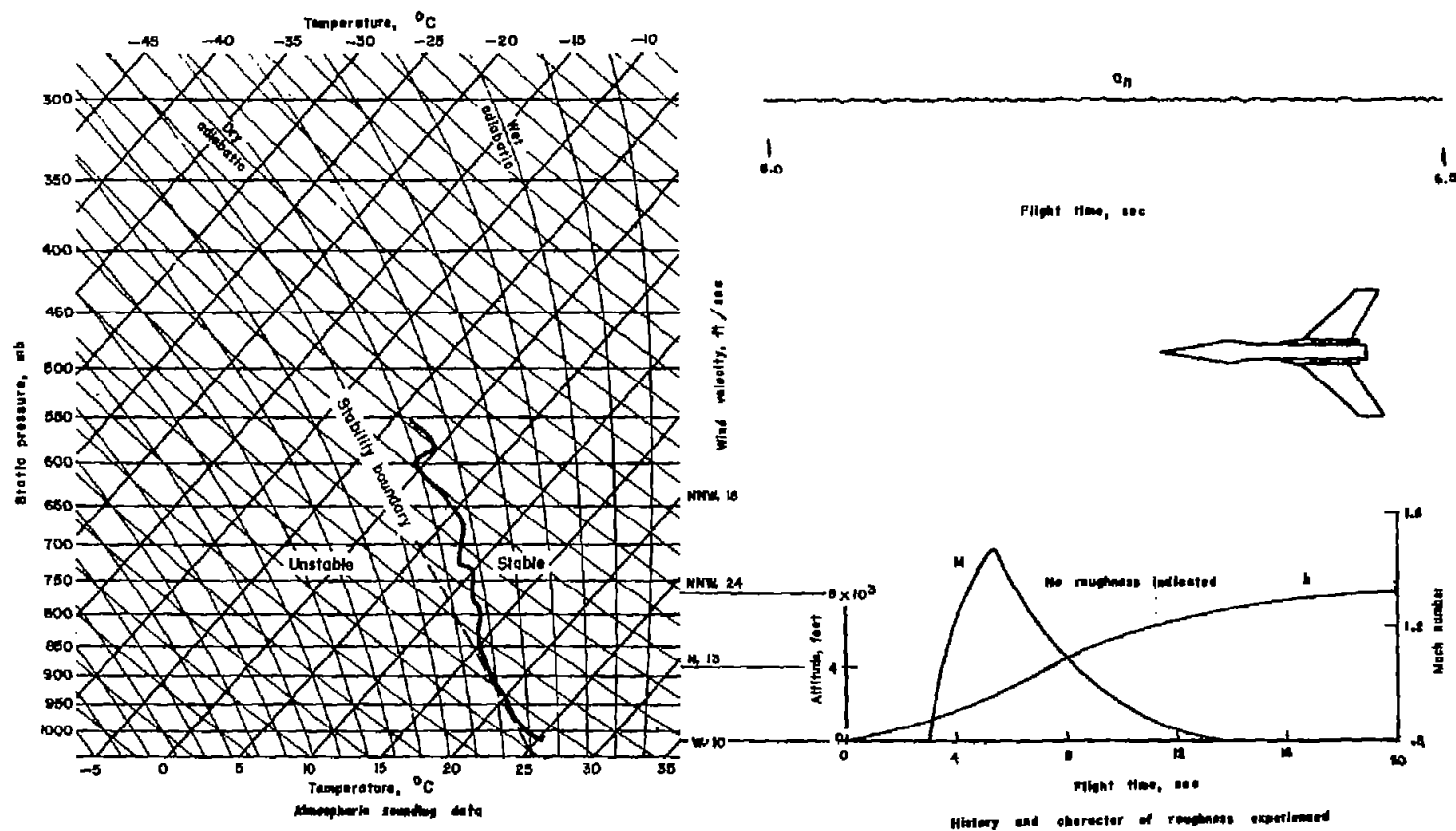


Figure 37.- Flight test made on July 25, 1955, with rawinsonde released at 3:45 p. m. (e. s. t.) and model launched at 3:22 p. m. (e. s. t.). Model wing loading, 22 lb/sq ft.

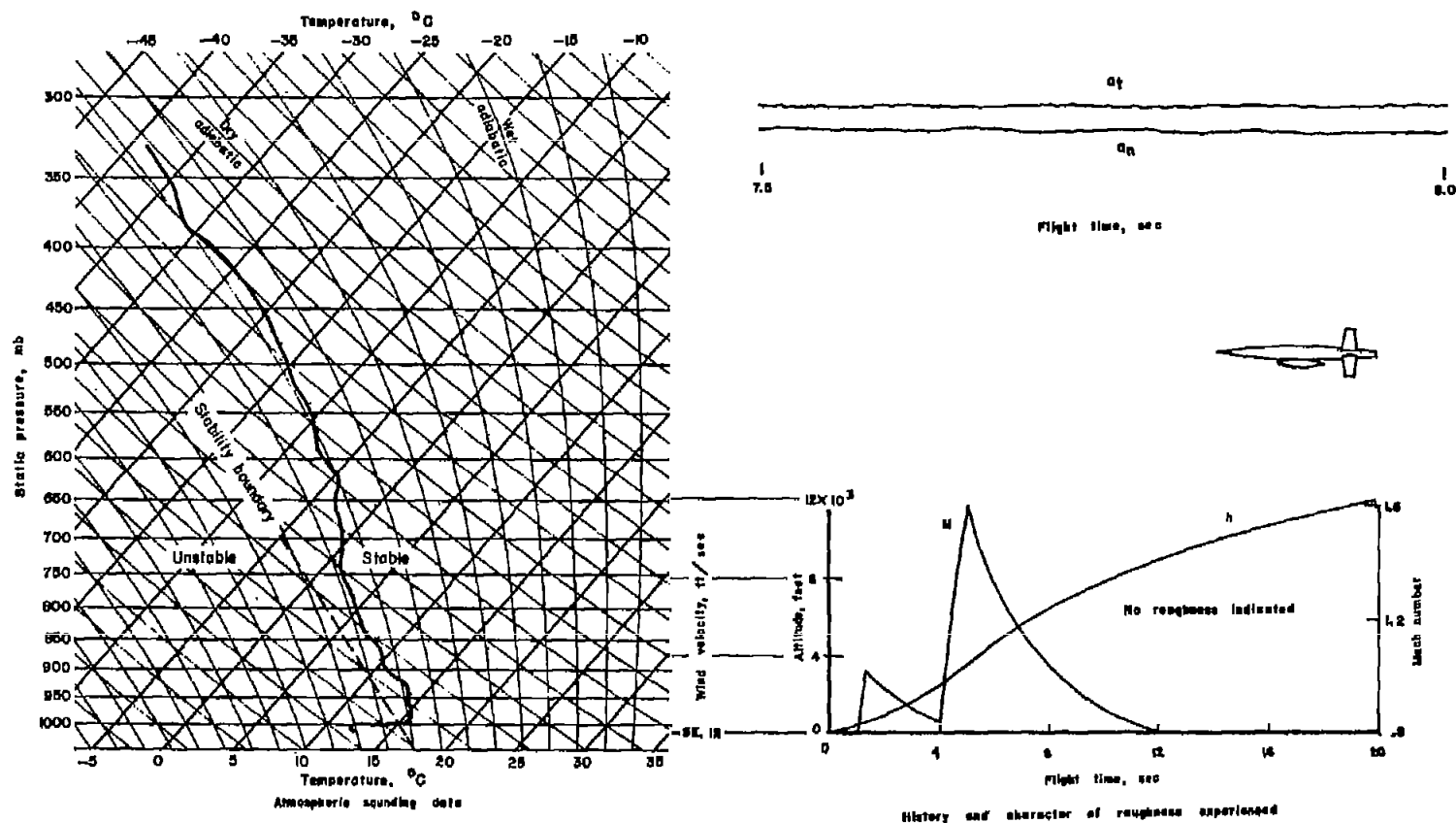


Figure 38.- Flight test made on December 10, 1952, with rawinsonde released at 1:42 p. m. (e. s. t.) and model launched at 1:22 p. m. (e. s. t.). Model wing loading, 50 lb/sq ft.